

RESEARCH

Open Access



Transcriptomic responses in the nervous system and correlated behavioural changes of a cephalopod exposed to ocean acidification

Jodi T. Thomas^{1,2*}, Roger Huerlimann², Celia Schunter³, Sue-Ann Watson^{1,4,5}, Philip L. Munday^{1,4} and Timothy Ravasi^{1,2}

Abstract

Background The nervous system is central to coordinating behavioural responses to environmental change, likely including ocean acidification (OA). However, a clear understanding of neurobiological responses to OA is lacking, especially for marine invertebrates.

Results We evaluated the transcriptomic response of the central nervous system (CNS) and eyes of the two-toned pygmy squid (*Idiosepius pygmaeus*) to OA conditions, using a *de novo* transcriptome assembly created with long read PacBio ISO-sequencing data. We then correlated patterns of gene expression with CO₂ treatment levels and OA-affected behaviours in the same individuals. OA induced transcriptomic responses within the nervous system related to various different types of neurotransmission, neuroplasticity, immune function and oxidative stress. These molecular changes may contribute to OA-induced behavioural changes, as suggested by correlations among gene expression profiles, CO₂ treatment and OA-affected behaviours.

Conclusions This study provides the first molecular insights into the neurobiological effects of OA on a cephalopod and correlates molecular changes with whole animal behavioural responses, helping to bridge the gaps in our knowledge between environmental change and animal responses.

Keywords Carbon dioxide, Climate change, Gene expression, Behaviour, Neurotransmission, Neuroplasticity, Immune, Oxidative stress

*Correspondence:

Jodi T. Thomas

jodi.thomas@my.jcu.edu.au

¹Australian Research Council Centre of Excellence for Coral Reef Studies, James Cook University, Townsville, QLD 4811, Australia

²Marine Climate Change Unit, Okinawa Institute of Science and Technology Graduate University, Okinawa, Japan

³Swire Institute of Marine Science, School of Biological Sciences, The University of Hong Kong, Pok Fu Lam Road, Hong Kong SAR, China

⁴College of Science and Engineering, James Cook University, Townsville, QLD 4811, Australia

⁵Biodiversity and Geosciences Program, Queensland Museum Tropics, Queensland Museum, Townsville, QLD 4810, Australia



© The Author(s) 2024. **Open Access** This article is licensed under a Creative Commons Attribution 4.0 International License, which permits use, sharing, adaptation, distribution and reproduction in any medium or format, as long as you give appropriate credit to the original author(s) and the source, provide a link to the Creative Commons licence, and indicate if changes were made. The images or other third party material in this article are included in the article's Creative Commons licence, unless indicated otherwise in a credit line to the material. If material is not included in the article's Creative Commons licence and your intended use is not permitted by statutory regulation or exceeds the permitted use, you will need to obtain permission directly from the copyright holder. To view a copy of this licence, visit <http://creativecommons.org/licenses/by/4.0/>. The Creative Commons Public Domain Dedication waiver (<http://creativecommons.org/publicdomain/zero/1.0/>) applies to the data made available in this article, unless otherwise stated in a credit line to the data.

Background

As human-induced environmental changes progress, establishing how animals respond to projected future environmental conditions, and why these responses occur, is critical [1]. A thorough understanding of why biological responses are occurring is especially useful for gaining insight into why some individuals or species are more sensitive to environmental change than others, and improving predictions of how organisms and populations will respond over the timescales at which environmental change is occurring [2]. The nervous system forms the fundamental link between the environment and animal's responses [3, 4]. Thus, the neurobiological impacts of anthropogenic environmental change are key to understanding how animals will respond as environmental change progresses, yet the role of the nervous system in biological responses to environmental change has been little explored [3].

The uptake of anthropogenic carbon dioxide (CO₂) by the ocean is causing seawater CO₂ levels to rise, decreasing seawater pH and altering the concentration of carbonate ions, in a process known as ocean acidification (OA) [5]. These chemical changes can fundamentally affect marine organisms and the ecosystems they inhabit [6]. OA affects a wide variety of physiological processes, life history traits and behaviours of marine invertebrates [7–11]. Invertebrates are vital components of marine ecosystems, comprising over 92% of species in the ocean, are essential to the function of ecosystem processes, and support the livelihoods of human societies across the globe [12, 13]. Animal behaviour influences an individual's own fitness, complex interactions with other individuals and species, and key ecological processes that shape the structure of marine communities and ecosystems [14]. Consequently, any behavioural effects of elevated CO₂ on marine invertebrates could potentially have wide-ranging ecological, social and economic consequences.

Despite many studies assessing the behavioural responses of marine invertebrates to OA the link between the environment and behavioural responses, the nervous system, has been largely understudied. The work that has addressed the neurobiological impacts of OA has focused on the functioning of GABA_A receptors. The GABA hypothesis was first proposed in fish and suggests acid-base regulatory mechanisms occurring at elevated CO₂ conditions alter ionic gradients across neuronal membranes, consequently disturbing GABA_A receptor function and causing behavioural alterations [15]. A range of research has supported the GABA hypothesis in fish (reviewed in Heuer, Hamilton [16]), and more recently pharmacological studies have also supported the GABA hypothesis in molluscs [17–19], but not a crustacean [20]. However, OA may also have a range of other neurobiological impacts, including altering the function of other

ligand-gated ion channels that are similar to the GABA_A receptor [18] and affecting synaptic plasticity [21, 22].

Transcriptomics provides a powerful non-targeted, holistic approach to identify functional responses to environmental change. Indeed, transcriptomics has widely been taken up by the OA research community to understand the response of marine animals to elevated CO₂ [23]. However, there is less research assessing the transcriptomic response of nervous tissue to elevated CO₂. Recently, studies have examined the transcriptomic response of the fish nervous system to elevated CO₂ conditions, including in coral reef fishes [24–28], temperate marine fishes [21, 29, 30] and ocean-phase salmon [31]. In marine invertebrates, two transcriptomic studies assessing the whole-body response of pteropod molluscs to elevated CO₂ identified altered expression of genes involved in nervous system function [32, 33]. However, whole body measurements cannot determine if non-tissue-specific transcripts are responding to elevated CO₂ in a system-wide manner, or only within specific tissues. Furthermore, due to the heterogeneity and complexity of gene expression, measurements at the whole-body level may mask transcriptomic responses in specific tissues, such as the nervous system.

Here, we investigated the transcriptomic response to OA in the central and peripheral nervous system of a cephalopod, the two-toned pygmy squid (*Idiosepius pygmaeus* [34]), and then correlated the molecular responses with behavioural changes recorded in the same individuals. Cephalopods have complex nervous systems and behaviours rivalling those of fishes [35], making them a useful taxon to investigate the neurobiological impacts of elevated CO₂. *I. pygmaeus* is a diurnal, tropical squid inhabiting shallow, inshore waters of the Indo-Pacific, including Northern and North-eastern Australia [36, 37]. They are a small, short-lived squid growing to a maximum mantle length of 2 cm [36], and have a lifespan of up to 80 days [38]. *I. pygmaeus* is an ideal species to use as previous research in this species found elevated CO₂ alters a range of behaviours [18, 39, 40].

In this study, we used RNA from the central nervous system (CNS) and eyes (peripheral sense organ) from squid exposed to current-day (~400 μatm) or elevated (~1,000 μatm) CO₂ levels for 7 days in a previous study by Thomas, Spady [18]. In these squid, elevated CO₂ exposure increased activity levels as well as visually-guided, conspecific-directed attraction and aggression [18]. Here, we created a *de novo* transcriptome assembly, providing a reference which we used to determine the transcriptomic response of the squid CNS and eyes to elevated CO₂. We used the eyes because cephalopods, including squid, are highly visual animals with many visually-guided behaviours [41–43]. Furthermore, we have shown elevated CO₂-induced disturbances of

visually-guided behaviour in the same squid used in this study [18]. As we had transcriptomic and behavioural data from the same individual squid, we also correlated patterns of gene expression with CO₂ treatment levels and OA-affected behaviours to determine key genes and processes in the cephalopod CNS and eyes potentially contributing to OA-induced behavioural changes. The results from this study help us understand, at a molecular level, the neurobiological impacts of ocean acidification in a marine invertebrate with a complex nervous system.

Methods

Animal collection and experimental setup

The squid tissues and behavioural data used in this study came from a previous experiment. Specifically, we used sham-treated squid from the picrotoxin experiment in Thomas, Spady [18] (Fig. 1). As described in Thomas, Spady [18], male two-toned pygmy squid (*Idiosepius pygmaeus*) were collected from the wild and acclimated in groups at current-day seawater conditions for 1–6 days before transferral to individual treatment tanks set

at either current-day (~400 μatm) or elevated (~1,000 μatm) CO₂ levels, consistent with CO₂ levels projected for 2100 following the representative concentration pathway RCP8.5 scenario [5]. Experiments were carried out in four interconnected 8,000 L recirculating seawater systems; two untreated seawater systems were used for current-day CO₂ treatments, and two seawater systems were dosed with CO₂ using a custom-built pH control system for elevated CO₂ treatments. The CO₂ conditions achieved were current-day CO₂: 407±58 μatm pCO₂, pH_T = 8.09±0.10 and elevated CO₂: 1,071±71 μatm pCO₂, pH_T = 7.73±0.03 (mean±SD). Refer to Thomas, Spady [18] for further details. CO₂ variation is common in coastal habitats [44]. However, the coastal waters where we collected *I. pygmaeus* show little daily variation in seawater pCO₂ levels; average daily range 20.3±8.6 μatm CO₂ (mean±SD) (Supplementary Text S1 and Figure S1). Thus, our experimental CO₂ levels are ecologically relevant to the population of *I. pygmaeus* used.

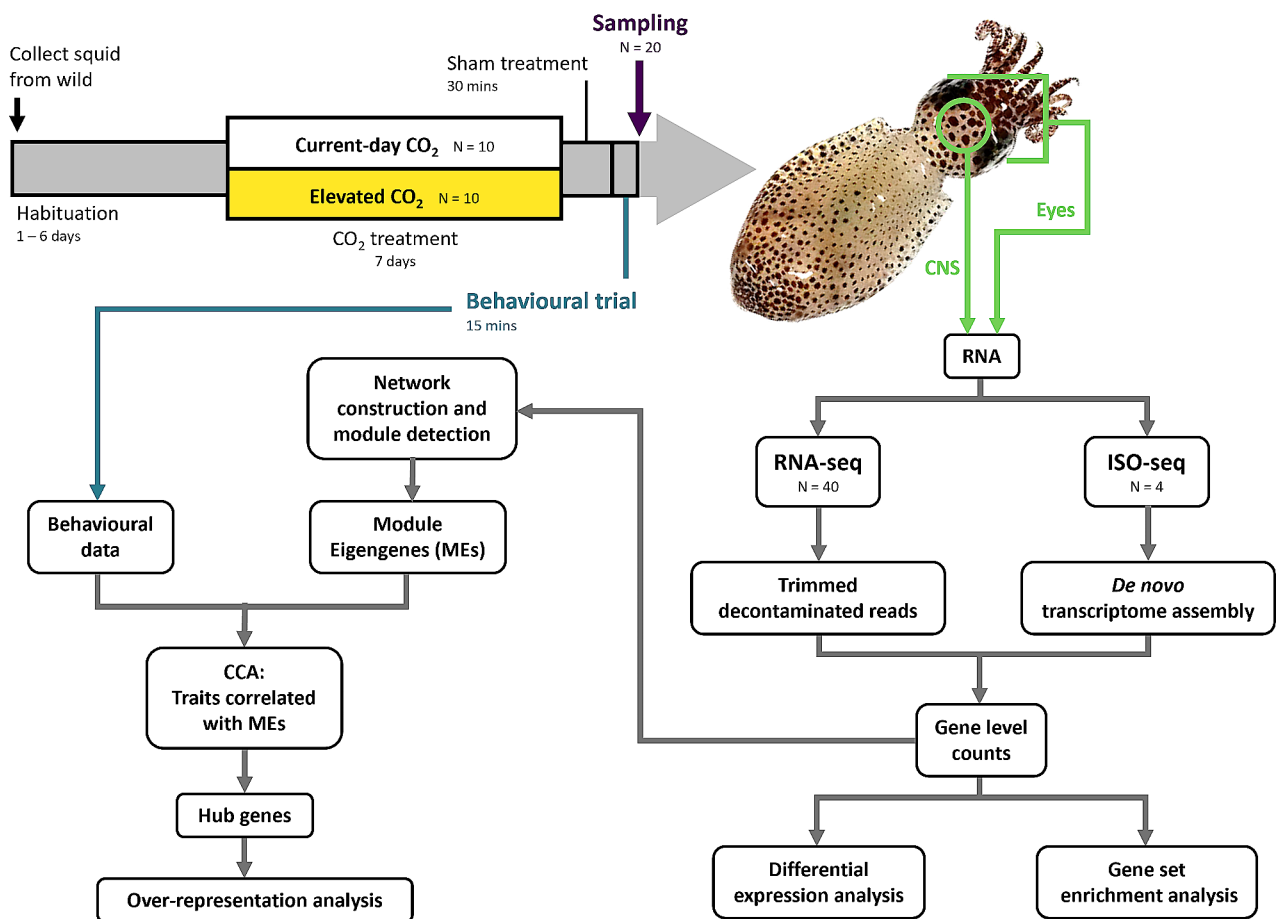


Fig. 1 Experimental design overview. CCA=canonical correlation analysis. *Idiosepius pygmaeus* photograph by Jodi Thomas

Behavioural analysis

After 7 days of current-day or elevated CO₂ treatment, squid underwent sham treatment by being individually placed in 100 mL of aerated seawater from their CO₂ treatment containing 0.2% ethanol for 30 min, as part of the experiment by Thomas, Spady [18]. Visually-guided behaviour was then tested for 15 min by placing squid individually in a tank (30×30×15 cm) filled to 3 cm depth with seawater from their CO₂ treatment and with a mirror taking up the entire area of one wall. Three aspects of squid behaviour shown to be altered by elevated CO₂ in Thomas, Spady [18], activity level, aggressive conspecific-directed behaviour and exploratory conspecific-directed behaviour (Table 1), were used here. See Thomas, Spady [18] for a detailed description of the behavioural analysis and results.

Tissue sample collection

Immediately after each behavioural trial, squid were euthanised with AQUI-S (1:1000). The head was separated from the mantle, rinsed in distilled water, and blotted dry. The skin, tentacles, beak, and buccal mass were removed and the eyes and central nervous system (CNS, containing the oesophagus running through the middle) were dissected and snap frozen in liquid nitrogen within 4.18±0.55 (mean±SD) minutes after euthanasia. Tissues were then transferred to -80°C for storage. This study was approved by and followed the animal ethics guidelines at James Cook University (JCU animal ethics number A2644).

Table 1 Squid behaviours shown to be altered by OA in Thomas, Spady [18]

Behaviour	CO ₂ Treatment Effect
Activity	
Active time (s)	↑
Total distance moved (cm)	↑
Average speed (cm/s)	↑
Visually-mediated aggressive conspecific-directed behaviour	
Proportion of squid displaying one or more aggressive interactions	↑
Number of aggressive interactions per individual	↑
Visually-mediated exploratory conspecific-directed behaviour	
Time spent in Zone A (3 cm closest to the mirror)	↑
Proportion of squid displaying one or more exploratory interactions	↑
Number of exploratory interactions per individual	↑

These behaviours are used alongside transcriptomic data from the same individual squid within the current study. ↑ = increase in the behaviour at elevated compared with current-day CO₂ conditions

RNA extraction

Total RNA was extracted from the entire CNS, and both eyes combined for each squid ($n_{\text{current-day CO}_2} = 10$, $n_{\text{elevated CO}_2} = 10$ for each tissue) (Fig. 1). Each tissue sample was homogenised in RLT-Plus Buffer (Qiagen) with sterile zirconia/silica beads (1 mm diameter, BioSpec Products) in a Mini-BeadBeater 96 (BioSpec Products) for a total of 2 min. Total RNA was extracted using an AllPrep DNA/RNA Mini Kit (Qiagen). RNA integrity of all 40 samples was measured on an Agilent 2200 TapeStation (High Sensitivity RNA ScreenTape, Agilent) (Supplementary File S1).

RNA sequencing

The Sequencing Section, Okinawa Institute of Science and Technology Graduate University, Japan carried out library preparation and sequencing on all 40 RNA samples. RNA was quantified by Qubit Flex Fluorometer (Qubit RNA BR assay kit, Thermo Fisher Scientific Inc.). The NEBNext® Poly(A) mRNA Magnetic Isolation Module (New England BioLabs Inc.) was followed according to the manufacturers protocol to isolate mRNA. One library was prepared for each sample, using the NEBNext® Ultra II Directional RNA Library Prep Kit for Illumina® (New England BioLabs Inc.) following the manufacturers protocol, using ten PCR cycles. Libraries were sequenced on two lanes of a NovaSeq6000 with a S2 flow cell paired end to the length of 150 bp.

RNA-seq read pre-processing

For a detailed workflow of the bioinformatic and statistical analyses, see Supplementary Figure S2. Raw reads were inspected with FastQC (v0.11.9) [45] and MultiQC (v1.9) [46] and trimmed with Fastp (v0.21.1) [47] using a sliding window of 4 bp, a mean Phred score of 30 and reads < 30 bp were trimmed. Kraken2 (v2.0.9) [48] was used with a confidence of 0.3 to remove any contamination using the NCBI bacterial and archaeal reference libraries (downloaded 08/2020).

Read mapping and counting

As a reference for gene expression quantification, we created and annotated a *de novo* transcriptome assembly of *I. pygmaeus* CNS and eye tissues using long read PacBio ISO-sequencing data. Refer to Supplementary Text S2 for a description of the methods for ISO-sequencing, *de novo* transcriptome assembly, and transcriptome annotation. The transcriptome assembly (fasta file) can be found at NCBI BioProject PRJNA798187 <https://www.ncbi.nlm.nih.gov/bioproject/?term=PRJNA798187> [49] and the annotated transcriptome assembly (OmicsBox and csv files) are available from DOI <https://doi.org/10.25903/ha66-mm11>.

[50]. The trimmed and decontaminated RNA-seq reads were mapped against the transcriptome assembly using salmon (v1.3.0) [51]. Correction for sequence-specific biases and fragment-level GC biases was used, the quantification step was skipped, and the flags ‘--validateMappings’ and ‘--hardFilter’ were also used. Corset (v1.09) [52] was run on the salmon equivalence class files from all 40 samples to cluster the transcripts to gene-level and produce gene-level counts. In Corset, we provided the four groups/treatments (eyes current-day CO₂, eyes elevated CO₂, CNS current-day CO₂ and CNS elevated CO₂), the log likelihood ratio test was switched off to prevent differentially expressed transcripts being split into different clusters, and the links between contigs were removed if the link was supported by less than 10 reads.

Statistical analyses

All statistical analyses (as described below) were carried out in R (v4.0.4) [53], primarily using RStudio (v 1.4.1106) [54].

Differential expression analysis

DESeq2 (v1.30.1) [55] using the Wald test was used to compare gene expression between current-day and elevated CO₂ conditions for the CNS and eyes separately. Genes with an adjusted p-value (padj, Benjamini-Hochberg method) < 0.05 were reported as differentially expressed (DE). Log2fold change estimates were shrunk with the ash method [56] to increase their accuracy.

Gene set enrichment analysis

Gene set enrichment analysis (GSEA) was run in clusterProfiler (v3.18.1) [57] for each tissue separately to determine if sets of genes from the same gene ontology (GO) term/functional category showed significant, concordant differences between current-day and elevated CO₂ conditions. Unweighted GSEA was run using the DESeq2 log₂ fold-change values of all genes and the annotated GO terms as the ‘gene sets’. A minimum and maximum gene set size of 15 and 500, respectively, was used. GSEA determines if genes from the same functional category are significantly more likely to occur at the top or bottom of the log₂ fold-change list and therefore whether these functional categories are up- or down-regulated at elevated CO₂, respectively. P-values were adjusted for multiple comparisons using the Benjamini-Hochberg method and a significance threshold of padj < 0.05 was used. The GSEA results were imported into Cytoscape (v3.8.2) [58] where EnrichmentMap (v3.3.1) [59] was used to create a network to visualise the functional enrichment results. All significant functional categories were included in the network as a circular node. Functional categories with > 0.25 similarity were linked by edges. Similar functional

categories were manually grouped into clusters and labelled.

Correlating gene expression profiles with CO₂ treatment and OA-affected behaviours

To analyse the correlation between gene expression and behavioural traits of squid across CO₂ treatments, we employed weighted gene co-expression network analysis (WGCNA) followed by canonical correlation analysis on the CNS and eyes, separately (Fig. 1). Refer to Supplementary Text S3 for a detailed description of the methods for gene co-expression network construction and module detection, module eigengene correlation with behavioural traits, module membership vs. gene significance, and identification of hub genes (Figures S3 – S21, Tables S1 and 2). Briefly, the gene-level counts from DESeq2 (v1.30.1) [55] were used in the WGCNA package (v1.70-3) [60] to construct a co-expression network and detect modules of genes. A module eigengene was calculated for each module of genes, representing the gene expression profiles of that module. Canonical correlation analysis using package CCA (v1.2.1) [61] was used to explore the correlations between the two sets of variables from the same individual squid: ME set = module eigengenes from each module; traits set = CO₂ level (current-day or elevated) and behavioural traits (active time (s), distance (cm), speed (cm/s), time in Zone A (s), whether the squid displayed an exploratory/aggressive interaction (yes/no), number of exploratory/aggressive interactions). For those modules identified by canonical correlation analysis to be correlated with each trait, the Pearson correlation of module membership (MM, higher value indicates the gene is more highly connected to the given module) and gene significance (GS, higher value indicates a more biologically relevant gene) was calculated [60]. A correlation of GS and MM implies that genes more highly connected with a given module also tend to be more highly correlated with the given trait, providing another measure for the importance of this module with the given trait [60]. This identified the final modules of interest, within which the MM and GS values of each gene were used as a screening method to identify biologically relevant, highly interconnected hub genes [60, 62, 63], i.e. to find genes correlated with CO₂ treatment and each behavioural trait. Hub genes were defined as those genes within the final modules of interest with a very strong correlation with the module (MM > 0.8) and a moderate correlation with the given trait (GS > 0.4).

All hub genes for CO₂ treatment were compared across tissues to identify hub genes for CO₂ treatment that are CNS-specific, eyes-specific or found in both tissues. Hub genes for CO₂ treatment that were also a hub gene for one or more behavioural traits were identified as genes correlated with the associated OA-induced behavioural

change. Finally, functional enrichment analysis was used for the CNS-specific CO₂ treatment hub genes that were also hub genes for all three activity traits in the CNS using over-representation analysis (ORA) in clusterProfiler (v3.18.1) [57] with the hypergeometric test. This determined if any GO terms were significantly over-represented within the list of hub genes. All other groups of CO₂ treatment hub genes had 25 or fewer genes and thus ORA was not used. P-values were adjusted for multiple comparisons using the Benjamini-Hochberg method and a significance threshold of padj<0.05 was used.

Results

Transcriptome assembly and annotation

The *de novo* transcriptome assembly for *Idiosepius pygmaeus* was created from a total of 138.6 million PacBio ISO-sequencing subreads and resulted in 49,981 transcripts that were clustered into 27,420 genes. The transcriptome assembly had an N50 of 3,163 bp, 70.4%

complete BUSCOs and an 82.1±5.5% overall alignment rate of the RNA-seq reads (Table S3). A total of 69% of the transcripts received a functional annotation (Supplementary Table S4). The species distribution of the top blast hits was dominated by cephalopod species (Figure S22). Final mapping of RNA-seq reads against the transcriptome assembly had a 73.6±6.9% mapping rate (Table S5).

Differentially expressed genes

We compared gene expression between current-day and elevated CO₂ conditions for the CNS and eyes separately. There was more variance in the eyes than the CNS (Fig. 2A). In the CNS, we identified 25 differentially expressed genes (DEGs) between current-day and elevated CO₂ conditions; 14 upregulated and 11 downregulated with elevated CO₂. In the eyes, there were eight DEGs; five upregulated and three downregulated at elevated, compared to current-day, CO₂ conditions (Fig. 2B).

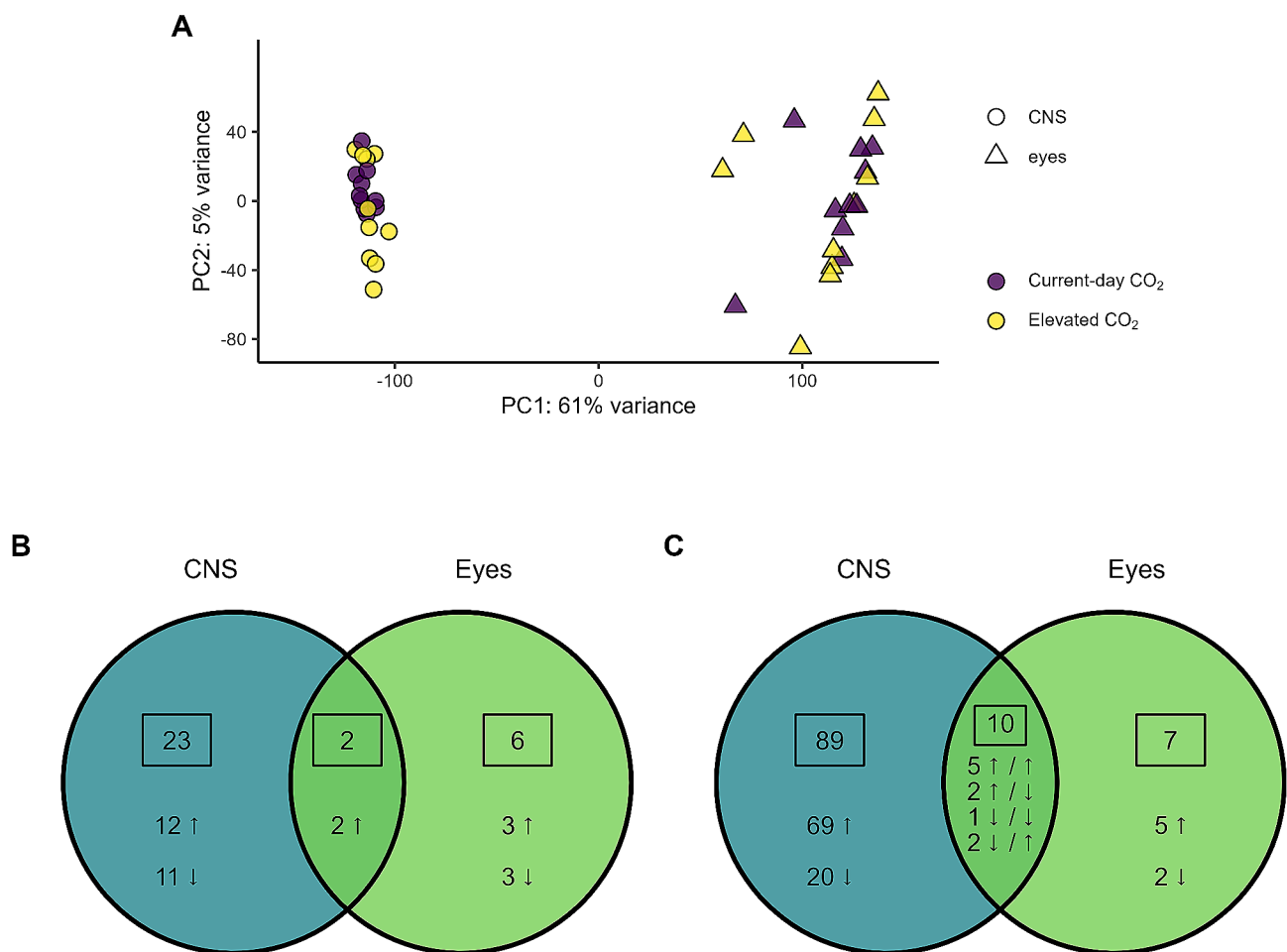


Fig. 2 Differential expression and GSEA results. **A** PC1 and PC2 axes from the principal components analysis of all genes for the 40 samples. **B** Venn diagram comparing the DEGs between current-day and elevated CO₂ levels in the CNS and eyes. **C** Venn diagram comparing the GO terms / functional categories found to be significantly different between current-day and elevated CO₂ levels in the CNS and eyes by GSEA. O = CNS, Δ = Eyes, ↑ = upregulated at elevated CO₂ conditions, ↓ = downregulated at elevated CO₂ conditions, purple = current-day CO₂, yellow = elevated CO₂.

See Figure S23 for a heatmap of all samples showing the expression pattern of all genes in the CNS and eyes, and Figure S24 for volcano plots of the CNS and eyes. Two genes were significantly upregulated with elevated CO₂ in both the CNS and eyes; one essential for autophagy (*ykt6*) and another poorly characterised gene (*fam204a*). In both tissues, the DEGs play roles in neurotransmission (CNS: *folh1, syvn1-b, slc2a13, celsr3*, eyes: *maoa, slc18a1, cbs*), immune function (CNS: *psenen, syvn1-b, map4k5, tf, nme6, map1l3ca/b*, eyes: *pglyrp2, cbs, maoa*), the oxidative stress response (CNS: *tf, cyb561d2, syvn1-b, chrac1, ykt6*, eyes: *cbs, ykt6*), and transcription regulation (CNS: *nme6, chrac1, znf271*, eyes: *gtf2e2*) (Table S6).

Small, coordinated changes in expression of genes belonging to the same functional categories

Gene set enrichment analysis (GSEA) identified Gene Ontology (GO) terms/functional categories, across all three GO categories (biological process, molecular function, and cellular component), that were significantly affected by CO₂ treatment, indicating small, coordinated changes in expression of the genes belonging to each of these functional categories. We identified ninety-nine significant functional categories in the CNS; 75 upregulated and 24 downregulated at elevated CO₂ (Fig. 2C).

These functional categories included those involved in transcription, RNA processing, translation, protein processing, the cell cycle and cell proliferation, and neurotransmission (Fig. 3 and S25). There were 17 significant functional categories in the eyes; 12 upregulated and 5 downregulated at elevated CO₂ (Fig. 2C). Ten functional categories were significantly affected by CO₂ treatment in both the CNS and eyes including functions related to the ribosome and translation, ion channels, kinase activity, protein degradation and cell adhesion (Fig. 3 and S25).

Genes correlated with OA-induced behavioural change

We identified 230 and 25 hub genes via for CO₂ treatment in the CNS and eyes, respectively, with 14 CO₂ treatment hub genes shared by both tissues. Of these CO₂ treatment hub genes in the CNS, eyes and both tissues, 169, 6 and 10 genes were also identified as hub genes for one or more behavioural traits, respectively, indicating these genes as potentially correlated with CO₂-induced behavioural changes (Fig. 4). Of the 169 genes in the CNS potentially contributing to CO₂-induced behavioural changes, 87 were positively correlated with CO₂ treatment and all three activity traits and were significantly enriched for 13 functional categories, including those playing a role in the cell cycle, cell migration, and protein

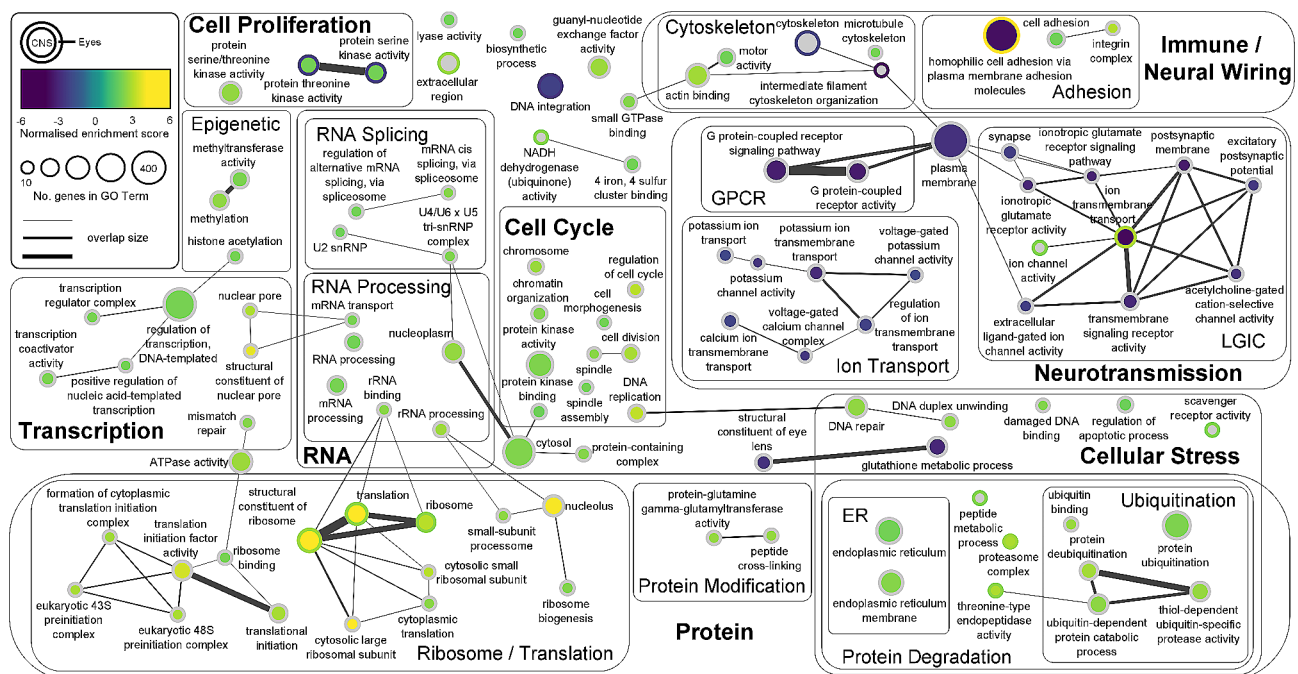


Fig. 3 Enrichment map displaying the gene set enrichment analysis (GSEA) results in both the CNS and eyes. Significant GO terms/functional categories are represented by a circular node. Results from the CNS and eyes are represented by colouration of the inner node area and node border, respectively. Yellow represents functional categories upregulated at elevated CO₂ and purple represents functional categories downregulated at elevated CO₂. Colour represents the normalised enrichment score and node size the number of core enrichment genes in each functional category. Functional categories found not significant (padj > 0.05) are coloured grey for the corresponding tissue type. The nodes from functional categories with a similarity > 0.25 are connected by an edge, with edge width increasing with increasing similarity (increasing number of genes shared by the functional categories). Similar functional categories were manually grouped into clusters and assigned a label

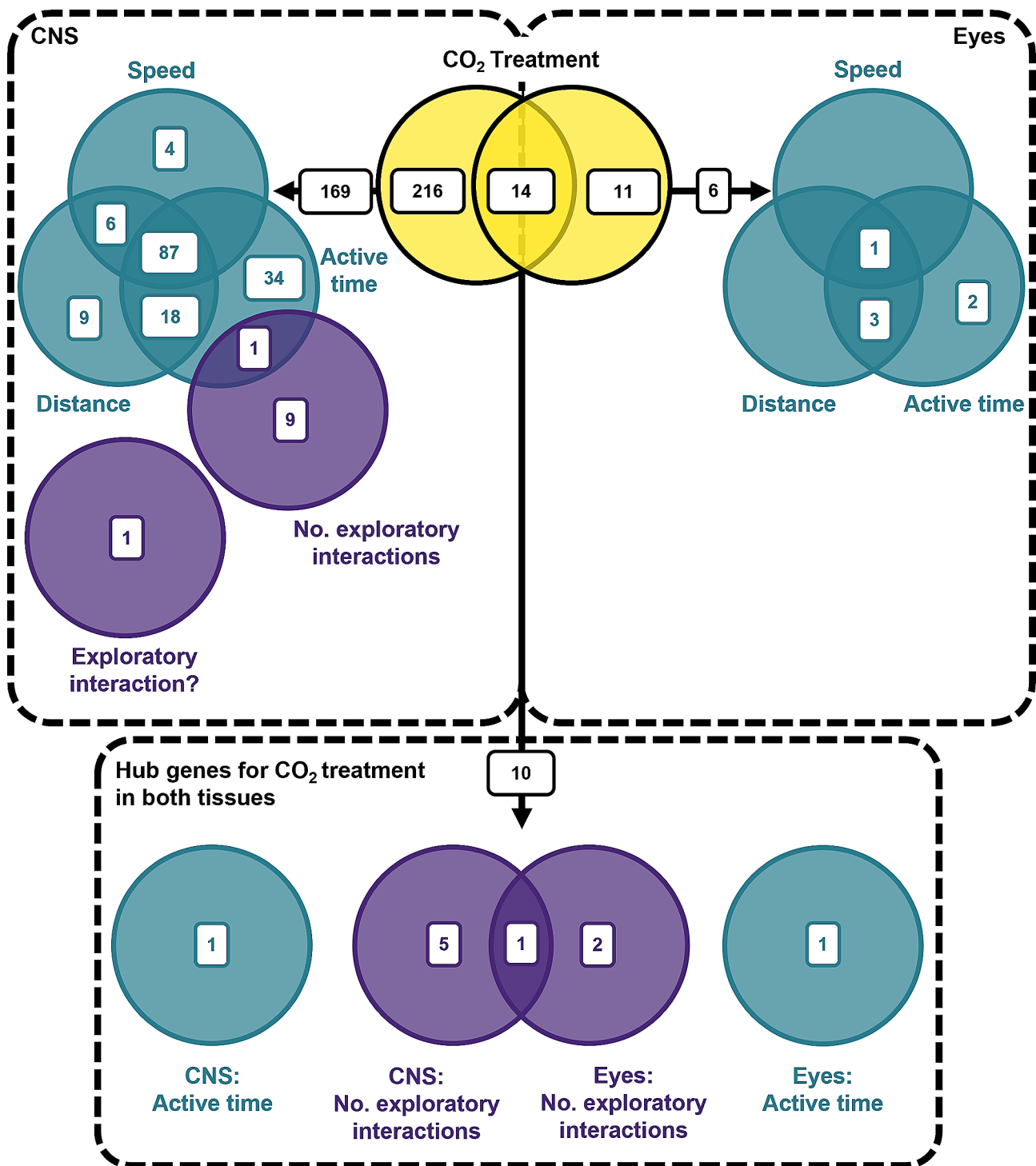


Fig. 4 Venn diagram depicting the number of hub genes identified for CO₂ treatment and behavioural traits in the CNS and eyes. The yellow Venn diagram in the centre depicts the number of hub genes for CO₂ treatment that are CNS-specific (left) and eyes-specific (right), and the overlap represents the number of CO₂ treatment hub genes shared by both tissues. CNS-specific and eyes-specific CO₂ treatment hub genes also identified as a hub gene for one or more behavioural traits in the CNS or eyes are on the left and right, respectively. Hub genes for CO₂ treatment found in both tissues, that are also a hub gene for a behavioural trait in one or both tissues, are shown at the bottom centre. CO₂ treatment hub genes shared with activity traits (active time, distance and speed) and exploratory conspecific-directed behaviours (number of exploratory interactions and whether any exploratory interactions occurred) are in teal and purple, respectively. Exploratory interaction? = whether any exploratory interactions occurred (yes/no)

synthesis and folding (Fig. 5). Four of these functional categories were also identified as significantly upregulated at elevated CO₂ in the CNS by GSEA; ‘nuclear pore’, ‘motor activity’, ‘chromosome’ and ‘protein kinase binding’. The 6 transcripts in the eyes potentially contributing to CO₂-induced behavioural changes had a match for two known genes; an acetylcholine receptor subunit (*chrna10*) and a gene essential for maintaining retinal tissue integrity (*crb*). The 10 transcripts in both tissues potentially contributing to CO₂-induced behavioural changes had a match for eight known genes, again including *chrna10*, and genes with putative roles in cell proliferation (*gid-4*, *cdk10*) and protein processing (*srp72*, *vhl*, *zranb1*). See Table S7 – S10 for all hub genes identified by WGCNA and their putative functions.

OA-affected genes and their functions

Genes affected by elevated CO₂ and correlated with OA-induced behavioural change were identified in seven main functions: neurotransmission; cell cycle; cell proliferation and differentiation; neural wiring; transcription,

RNA processing and protein processing; immune function; oxidative stress.

Neurotransmission

A range of genes and functional categories involved in various types of neurotransmission were significantly affected by CO₂ treatment (Table 2). We identified small, coordinated downregulation of genes belonging to a cluster of nine functional categories in the CNS, and upregulation of two functional categories in the eyes, involved in ligand-gated ion channel-mediated neurotransmission. The genes contributing most to the up-/down-regulation of each of these functional categories (core enrichment genes) in the CNS and eyes included genes for components of acetylcholine, GABA_A and glutamate ion channel receptors (Table S11). There was also small, coordinated downregulation in the CNS of genes belonging to two functional categories involved in G protein-coupled receptor (GPCR)-mediated neurotransmission, including genes coding for components of metabotropic glutamate, GABA_B, serotonin and dopamine receptors (Table S12). Notably, a subunit of nicotinic acetylcholine

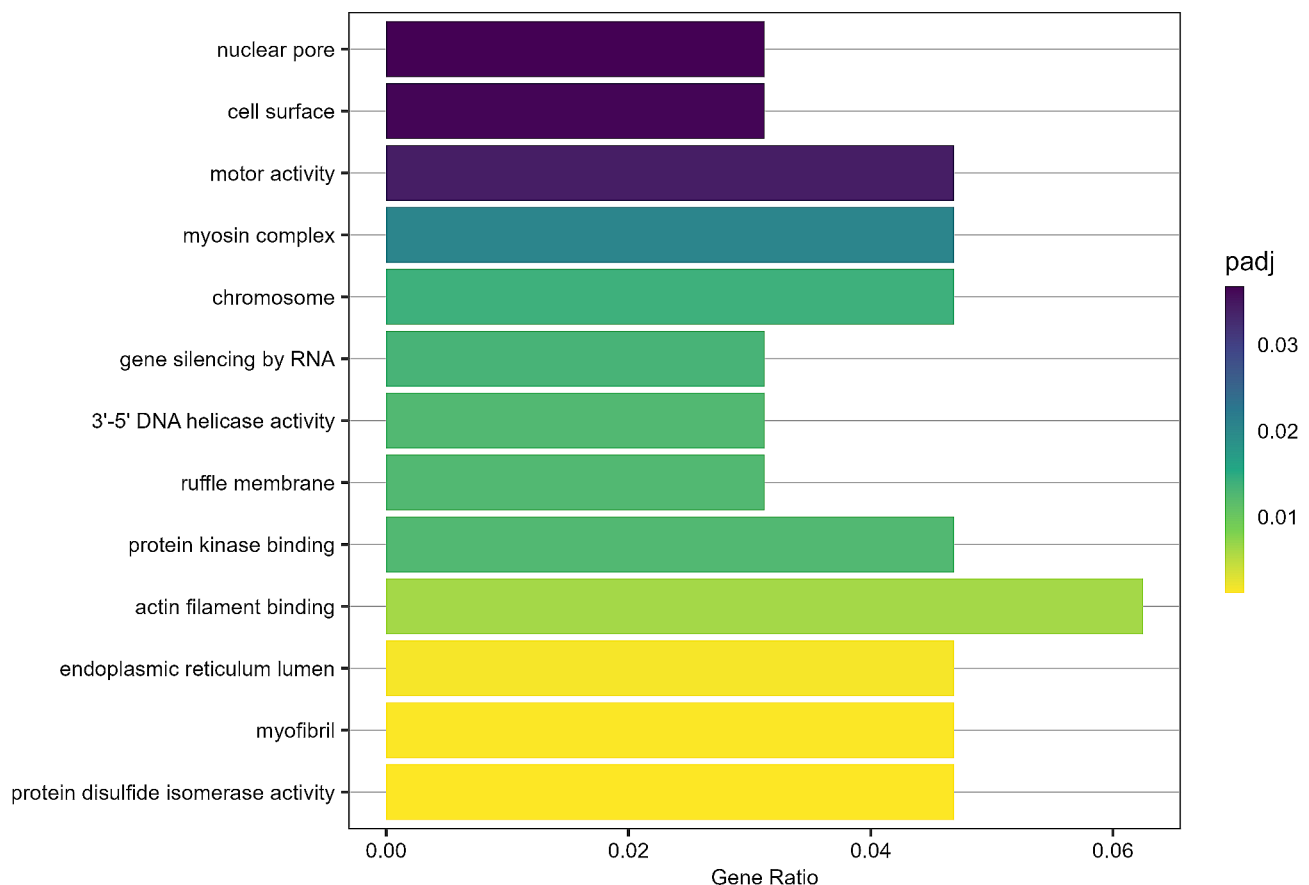


Fig. 5 GO Terms/functional categories significantly enriched from the 87 genes positively correlated with CO₂ treatment and all three activity traits in the CNS. Functional categories are ordered by their adjusted p-value. padj = adjusted p-value, yellow indicates a lower adjusted p-value / higher significance. Gene Ratio = the number of genes represented in the genes positively correlated with CO₂ treatment and all three activity traits in the CNS, in comparison to all of the genes in the CNS.

Table 2 Results across all three analysis methods in the CNS and eyes related to neurotransmission

	DE		GSEA			WGCNA				
	Gene	CNS	Eyes	GO Term / Functional Category	CNS	Eyes	Gene		Eyes	
							CO ₂	Behaviour	CO ₂	Behaviour
Neurotransmission										
Cholinergic										
				'acetylcholine-gated cation-selective channel activity', 'synapse*', 'postsynaptic membrane*', 'excitatory postsynaptic potential*', 'transmembrane signaling receptor activity*', 'extracellular ligand-gated ion channel activity*'	↓		<i>chrna10</i>	↓	↑	↑/↓ ↓
				'ion transmembrane transport*'	↓	↑				
				'ion channel activity*'		↑				
GABAergic	<i>syvn1-b</i>	↑		'extracellular ligand-gated ion channel activity*', 'G protein-coupled receptor signaling pathway*'	↓		<i>phf24</i> , <i>rac1</i>	↑	↑	
	<i>slc18a2</i>		↑	'ion transmembrane transport*'	↓	↑	<i>aldh5a1</i>	↓	↓	
Glutamatergic	<i>folh1</i>	↑		'ionotropic glutamate receptor signalling pathway', 'ionotropic glutamate receptor activity', 'synapse*', 'postsynaptic membrane*', 'G protein-coupled receptor signaling pathway*', 'G protein-coupled receptor activity*'	↓					
	<i>celsr3</i>	↓		'ion transmembrane transport*'	↓	↑				
				'ion channel activity*'		↑				
Monoaminergic	<i>maoa</i> , <i>slc18a2</i>		↑	'G protein-coupled receptor signaling pathway*', 'G protein-coupled receptor activity*'	↓					
General Processes for Synaptic Neurotransmission				'potassium channel activity', 'potassium ion transmembrane transport', 'voltage-gated potassium channel activity', 'regulation of ion transmembrane transport', 'voltage-gated calcium channel complex', 'calcium ion transmembrane transport'	↓	↓	<i>futsch</i> , <i>dgkq</i>	↓	↓	
GPCR Trafficking							<i>tmed2</i>	↑	↑	

Genes identified as significantly differentially expressed (DE) between current-day and elevated CO₂ conditions, GO Terms/functional categories significantly affected by elevated CO₂ treatment as identified by gene set enrichment analysis (GSEA), and genes identified as correlated with both CO₂ treatment and one or more OA-affected behaviours by weighted gene co-expression network analysis (WGCNA). DE: ↑ or ↓ = significant upregulation or downregulation of this gene at elevated compared to current-day CO₂ conditions. GSEA: ↑ or ↓ = significant upregulation or downregulation of this GO Term/functional category, indicating small, coordinated upregulation or downregulation of the genes belonging to this functional category, at elevated compared to current-day CO₂ conditions. WGCNA: CO₂ ↑ or ↓ = positive or negative correlation between the expression of the gene and CO₂ treatment, Behaviour ↑ or ↓ = positive or negative correlation between the expression of the gene and 1 or more OA-affected behaviours, ↑/↓ = different transcripts of the same gene were found to be positively and negatively correlated. * = GO Term contains core enrichment genes for this type of neurotransmission

receptors (*chrna10*) was correlated with CO₂ treatment and behaviours in both tissues. *Chrna10* as well as other genes coding for nicotinic acetylcholine receptor subunits (*chrna1*, *chrna3*, *chrna5*, and *chrbn1*) were core enrichment genes in eight functional categories significantly affected by CO₂ treatment in both tissues. Genes coding for regulation of GABAergic neurotransmission were upregulated in both tissues (CNS: *syvn1-b*, eyes: *slc18a2*), and positively correlated with CO₂ treatment and behaviours in the CNS (*phf24*, *rac1*), while *aldh5a1*, which is involved in the final degradation step of GABA [64], was negatively correlated with CO₂ treatment and

behaviours in the CNS. Furthermore, there was upregulation of *folh1* (glutamate synthesis) and downregulation of *celsr3* (mediator of glutamatergic synapse formation) in the CNS. There was also upregulation in the eyes of two key genes involved in monoaminergic (dopamine, serotonin (5-HT), norepinephrine, and epinephrine) neurotransmission (*maoa*, *slc18a2*).

Genes involved in the general processes required for synaptic neurotransmission also displayed altered expression after elevated CO₂ exposure (Table 2). There was small, coordinated downregulation in the CNS of genes belonging to a cluster of seven functional categories

involved in K^+ , Ca^{2+} and Na^+ ion transport important for general processes involved in neurotransmission, including maintenance of membrane potential, action potential generation and neurotransmitter release (Table S13). Furthermore, genes involved in regulating synaptic neurotransmission (*futsch*, *dgkq*) were negatively correlated with CO_2 treatment and activity traits in the CNS.

Cell cycle

In the CNS, we found small, coordinated upregulation of genes belonging to functional categories involved in the cell cycle, and genes positively correlated with CO_2 treatment and all three activity traits were enriched for cell cycle functional categories (Table 3; Figs. 3 and 5). This included genes and functional categories involved in regulating the cell cycle, as well as those specifically involved in the cell cycle stages of interphase and mitosis. In particular, there was small, coordinated upregulation of genes belonging to the functional categories 'chromosome' and 'protein kinase binding' (Fig. 3), and these same functions were enriched in the genes positively correlated with CO_2 treatment and all three activity traits (Fig. 5).

Cell proliferation and differentiation

Genes involved in cell proliferation and differentiation, including specifically for neuronal differentiation and neurogenesis were mostly positively correlated with CO_2 treatment and behaviours in the CNS (Table 3). Genes involved in neuronal differentiation (*ttc3*), neural stem cell self-renewal (*srvt*), neural progenitor proliferation (*melk*), and neurogenesis (*ncaph*, *adgrb3*) were all positively correlated with CO_2 treatment and activity traits. *Bcar3*, which promotes cell proliferation, migration and redistribution of actin fibres, and *psap*, which acts as a neurotrophic and myelintrophic factor, were negatively correlated with CO_2 treatment and positively correlated with number of exploratory interactions in the CNS. Several *cdk10* transcripts were identified as correlated with CO_2 -induced behavioural change. *Cdk10* codes for a protein kinase that plays pivotal roles in controlling a range of fundamental cellular processes including cell proliferation and neurogenesis (reviewed in Guen, Gamble [65]).

Neural wiring

A range of genes and functional categories involved in neural wiring, including cell migration and adhesion, and neurite growth and synapse formation were affected by CO_2 treatment, also mostly exhibiting an upregulation in the CNS (Table 3). There was small, coordinated upregulation of genes involved in cell migration functional categories, including 'motor activity', 'actin binding', 'cell adhesion' and 'integrin complex'. Those genes positively correlated with CO_2 treatment and all three activity traits

in the CNS were enriched for similar functional categories: 'actin filament binding', 'myosin complex', 'myofibril', 'motor activity' and 'ruffle membrane'. Genes with a role specifically in neuron migration and adhesion, and the related processes of dendrite and axon outgrowth and branching, dendritic spine formation, and synapse formation were also positively correlated with CO_2 treatment and activity (*rac1*, *ptpr*, *adgrb3*, *apbb1*). One gene involved in neurite growth and branching (*futsch*) was negatively correlated with CO_2 treatment and activity traits.

Transcription, RNA processing, and protein processing

There was generally an upregulation of genes and functional categories involved in transcription, RNA processing and protein processing in the CNS, and to a smaller extent in the eyes (Table 4). In the CNS, there was small, coordinated upregulation of genes belonging to functional categories involved in transcription, including 'DNA duplex unwinding', and its' daughter term '3'-5' DNA helicase activity' was enriched in those genes positively correlated with CO_2 treatment and all three activity traits (Fig. 5). There was small, coordinated upregulation in the CNS of genes belonging to the functional category 'nuclear pore', and 'nuclear pore' was also enriched for those genes positively correlated with CO_2 treatment and all three activity traits in the CNS (Fig. 5). Genes involved in transcription were also DE; *nme6*, *chrac1* and *znf271* were upregulated in the CNS, and *gtf2e2* downregulated in the eyes. There was small, coordinated upregulation of genes involved in 'RNA processing', 'mRNA processing' and 'rRNA processing', as well as functional categories involved in the processes and components of the spliceosome, which excises introns to produce mature mRNA (Fig. 3). Components of the spliceosome (*snrpa*, *snrnp200*) were also identified as correlated with CO_2 treatment and behaviours (Table 4).

A range of genes and functional categories involved in protein synthesis, folding and degradation/turnover were significantly upregulated in the CNS, and some were also upregulated in the eyes. Small, coordinated upregulation of genes involved in the initiation and process of translation as well as in functional categories for ribosomal components occurred in both tissues (Fig. 3). Genes with similar functions were also positively correlated with CO_2 treatment and activity traits in the CNS, including translation initiation factors (*eif3b*, *eif3d*), an elongation factor (*eef1g*), and ribosomal components (*rpl23a*, *rpl4*, *rpl7l*, *rps27a*). Genes involved in protein translocation (*stt3a*, *rpn1*, *rpn2*, *tmed2*), and protein folding and quality control (*pdia3*, *pdia4* and *pdia5*, *hspa5*) were correlated with CO_2 treatment and behaviours in the CNS. The endoplasmic reticulum associated degradation (ERAD) pathway involves protein ubiquitination followed by proteasomal

Table 3 Results across all methods related to the cell cycle, cell proliferation and differentiation, neural wiring

	DE			GSEA			WGCNA					
	Gene	CNS	Eyes	GO Term / Functional Category	CNS	Eyes	Gene	CNS		Eyes		
								CO ₂	Behaviour	CO ₂	Behaviour	
Cell cycle												
Interphase: G1 phase							<i>cdt1, snd1</i>	↑	↑			
Interphase: S phase				'DNA replication'	↑		<i>tubg1, nat10, psf2, cdt1, mcm5, dbf4, spt16, foxm1, bptf</i>	↑	↑			
Interphase: G2 phase							<i>ranbp2, donson</i>	↑	↑			
Mitosis				'chromosome,'chromatin organization'	↑		<i>ncaph, smc4, ttk, incenp, bub1, foxm1, cdt1</i>	↑	↑			
				'spindle,'spindle assembly'	↑		<i>bub3</i>	↑	↑			
				'cell division'	↑		<i>zip, myh9/10, myl9, anln, prpf40a</i>	↑	↑			
Cell cycle regulation				'regulation of cell cycle,'protein kinase binding,'protein kinase activity'	↑		<i>foxm1, eif3b, ccnb3, melk, ttk, bub1, dbf4, anb32a, klf10, ecd</i>	↑	↑			
							<i>stk10, calm</i>	↓	↓			
Cell proliferation and differentiation												
Cell proliferation				'protein serine/threonine kinase activity'	↑		<i>ttk, eif3b, foxm1, melk, dbf4, srrt, tk1, tgfb1i1, pa2g4, ttc3, ptp</i>	↑	↑			
				'protein serine kinase activity,'protein threonine kinase activity'	↑	↓	<i>gid-4</i>	↑		↑	↓	
							<i>bcar3</i>	↓	↑			
Cell differentiation							<i>eif3b, rac1, ptp, tbc1d1, tgfb1i1, itga4, pa2g4, slc4a11</i>	↑	↑			
							<i>btg1</i>	↓	↓			
Neuronal differentiation							<i>ttc3, rac1</i>	↑	↑			
Neurogenesis							<i>ncaph</i>	↑	↑			
							<i>cdk10</i>	↑/↓	↓		↓ ↑	
Neural Wiring												
Cell migration				'motor activity,'actin binding'	↑		<i>arpc5, anln, myl9, slit3, mbtp, prpf40a</i>	↑	↑			
							<i>dag</i>	↓	↓			
							<i>zranb1</i>	↓	↑		↓ ↑	
Cell adhesion				'cell adhesion,'integrin complex'	↑		<i>itga4, itga9, slc4a11, pcdh1, vcl, rac1, ptp, pa2g4</i>	↑	↑			
				'homophilic cell adhesion via plasma membrane adhesion molecules'	↓	↑	<i>pcdh1</i>	↓	↓			
Neurite growth and synapse formation							<i>adgrb3, rac1, apbb1, ptp</i>	↑	↑			
							<i>futsch</i>	↓	↓			

Results are shown for all three analysis methods in the CNS and eyes. Genes identified as significantly differentially expressed (DE) between current-day and elevated CO₂ conditions, GO Terms / functional categories significantly affected by elevated CO₂ treatment as identified by gene set enrichment analysis (GSEA), and genes identified as correlated with both CO₂ treatment and one or more OA-affected behaviours by weighted gene co-expression network analysis (WGCNA). See Table 2 for a description of the symbols

Table 4 Results across all methods related to transcription, RNA processing and protein processing

	DE		GSEA				WGCNA					
	Gene	CNS	Eyes	GO Term / Functional Category		CNS	Eyes	Gene	CNS		Eyes	
									CO ₂	Behaviour	CO ₂	Behaviour
Transcription	<i>chrac1,</i> <i>znf271</i>	↑		'DNA duplex unwinding','nuclear pore','regulation of transcription, DNA-templated','positive regulation of nucleic acid-templated transcription','transcription regulator complex','transcription coactivator activity'		↑		<i>polr1a,</i> <i>spt16, bptf,</i> <i>arpc5,</i> <i>nup160,</i> <i>nup155,</i> <i>nup205</i>	↑	↑		
	<i>nme6,</i> <i>gtf2e2</i>	↓										
RNA												
RNA Processing				'RNA processing','mRNA processing','rRNA processing','mRNA transport','rRNA binding'		↑		<i>cstf1,</i> <i>exosc10,</i> <i>nat10,</i> <i>pa2g4</i>	↑	↑		
RNA Splicing				'regulation of alternative mRNA splicing, via spliceosome','mRNA cis splicing, via spliceosome','U2snRNP','U4/U6 x U5 tri-snRNP complex'		↑		<i>melk,</i> <i>snrpa, ecd,</i> <i>prpf40a</i>	↑	↑		
								<i>snrnp200</i>	↑/↓	↑/↓		
Protein Translation				'translation'		↑	↑	<i>EIF3B, EIF3D,</i> <i>EEF1G</i>	↑	↑		
				'translation initiation','translation initiation factor activity','eukaryotic 48S preinitiation complex','eukaryotic 43S preinitiation complex','formation of cytoplasmic translation initiation complex','cytoplasmic translation'		↑						
Ribosome				'ribosome','structural constituent of ribosome'		↑	↑	<i>rpl23a,</i> <i>rpl4, rpl7,</i> <i>rps27a,</i> <i>nop58</i>	↑	↑		
				'cytosolic small ribosomal subunit','cytosolic large ribosomal subunit','small-subunit processome','ribosome biogenesis','ribosome binding'		↑						
Endoplasmic reticulum Protein trafficking				'endoplasmic reticulum','endoplasmic reticulum membrane'		↑		<i>STT3A,</i> <i>TMED2,</i> <i>RPN2, RPN1</i>	↑	↑		
								<i>SRP72</i>	↓		↓	↑
Protein modification				'peptide cross-linking','protein-glutamine gamma-glutamyltransferase activity'		↑						
Protein folding								<i>hspa5,</i> <i>pdia3,</i> <i>pdia4,</i> <i>pdia5, ssr1,</i> <i>ganab,</i> <i>ppib</i>	↑	↑		

Table 4 (continued)

	DE			GSEA			WGCNA					
	Gene	CNS	Eyes	GO Term / Functional Category	CNS	Eyes	Gene	CNS		Eyes		
								CO ₂	Behaviour	CO ₂	Behaviour	
Protein degradation: ubiquitination and proteasome	<i>syvn1-b</i>	↑		'proteasome complex'	↑	↑	<i>rpn1, ttc3, cblb</i>	↑	↑			
				'peptide metabolic process'		↑	<i>vhl</i>	↓	↑		↓	
				'protein ubiquitination','protein deubiquitination','ubiquitin binding','ubiquitin-dependent protein catabolic process','thiol-dependent ubiquitin-specific protease activity'	↑		<i>derl1</i>	↓	↑			
Protein degradation: lysosomal	<i>ykt6</i>	↑	↑				<i>tmcc1/2</i>	↓	↓			

Results are shown for all three analysis methods in the CNS and eyes. Genes identified as significantly differentially expressed (DE) between current-day and elevated CO₂ conditions, GO Terms/functional categories significantly affected by elevated CO₂ treatment as identified by gene set enrichment analysis (GSEA), and genes identified as correlated with both CO₂ treatment and one or more OA-affected behaviours by weighted gene co-expression network analysis (WGCNA). See Table 2 for a description of the symbols

Table 5 Results across all analysis methods in the CNS and eyes related to the immune response

	DE			GSEA			WGCNA					
	Gene	CNS	Eyes	GO Term / Functional Category	CNS	Eyes	Gene	CNS		Eyes		
								CO ₂	Behaviour	CO ₂	Behaviour	
Immune Sensor	<i>pglyrp2</i>		↓	'scavenger receptor activity'		↑						
Immune signalling pathways	<i>map4k5/3, syvn1-b</i>	↑					<i>abhd12</i>	↑	↑			
	<i>psenen</i>		↓									
	<i>cbs, maaa</i>		↑									
Effector: Controlling resources required by pathogens	<i>tf, nme6</i>	↑					<i>tf</i>	↑	↑			
Effector: Autophagy	<i>map1b3ca/b</i>		↓									
Effector: Phagocytosis				'cell adhesion','integrin complex','motor activity','actin binding','microtubule cytoskeleton'	↑		<i>itga4, itga9, rac1, ptptr</i>	↑	↑			
				'cytoskeleton','intermediate filament cytoskeleton organisation'		↓						

Genes identified as significantly differentially expressed (DE) between current-day and elevated CO₂ conditions, GO Terms/functional categories significantly affected by elevated CO₂ treatment as identified by gene set enrichment analysis (GSEA), and genes identified as correlated with both CO₂ treatment and one or more OA-affected behaviours by weighted gene co-expression network analysis (WGCNA). See Table 2 for a description of the symbols

degradation and we found a range of genes involved in this process to be affected by CO₂ treatment. There was small, coordinated upregulation of genes in the 'endoplasmic reticulum' and five ubiquitin-related functional categories in the CNS, of 'proteasome complex' in both tissues, and of 'peptide metabolic process' in the eyes. Genes positively correlated with CO₂ treatment and all three activity traits were enriched for 'endoplasmic reticulum lumen' and included genes coding for E3 ubiquitin ligases (*cblb, ttc3*) and a subunit for the 26S proteasome (*rpn1*). A gene coding for an E3 ubiquitin ligase (*syvn1-b*) was also upregulated in the CNS. Lysosomal degradation

is another method for protein turnover, and a gene essential for lysosomal function (*ykt6*) was upregulated in both the CNS and eyes.

Immune function

Genes and functional categories involved in the three stages of the innate immune response (sensing, signalling and effectors), were affected by CO₂ treatment in both tissues (Table 5). In the eyes, the immune sensor molecule *pglyrp2* was downregulated, while there was small, coordinated upregulation of genes belonging to the functional category 'scavenger receptor activity' which binds

pathogens. Genes that mediate the immune response via cellular signalling pathways were DE, including upregulation of *map4k5/3* and *syvn1-b*, and downregulation of *psemen* in the CNS. In the eyes, there was upregulation of *maoa*, which plays a key role, via norepinephrine signalling, in the molluscan neuroendocrine-immune axis-like pathway [66–68]. Genes involved in the activation and production of immune effectors were also affected by CO₂ treatment. In particular, *tf* coding for transferrin, which sequesters iron so it is unavailable for pathogens and is a key component of the molluscan innate immune response, including in squid [69–73], was upregulated and positively correlated with CO₂ treatment and activity traits in the CNS. The key molecular marker of autophagy, *map113ca/b*, which plays an important role in the molluscan immune response [74–76] was downregulated in the CNS. There was also small, coordinated upregulation of genes belonging to functional categories involved in mediating phagocytosis, including ‘cell adhesion’ and ‘integrin complex’. Genes involved in cell adhesion as part of the immune response (*itga4*, *itga9*, *rac1*, *ptpr*) were also positively correlated with CO₂ treatment and activity traits. The cytoskeleton is also important for phagocytosis and there was small, coordinated upregulation of genes in three cytoskeleton-related functional categories in the CNS (‘motor activity’, ‘actin binding’, and

‘microtubule cytoskeleton’), and two downregulated in the eyes (‘cytoskeleton’ and ‘intermediate filament cytoskeleton organisation’) (Fig. 4).

Oxidative stress

Genes involved in regulating reactive oxygen species (ROS) and antioxidant production were differentially expressed in both issues; *tf* (CNS: upregulated and positively correlated with CO₂ treatment and activity traits), *cyb561d2* (CNS: downregulated), *cbs* (eyes: upregulated). Furthermore, *scl4a11*, which regulates the oxidative stress response, was positively correlated with CO₂ treatment and activity traits in the CNS, and there was small, coordinated downregulation in the CNS of genes involved in ‘glutathione metabolic process’ (Table 6). Genes and functional categories involved in response to oxidative damage were also affected by CO₂ treatment (Table 6). Genes involved in DNA repair were generally upregulated with CO₂ treatment in the CNS; *chrac1* was significantly upregulated, there was small, coordinated upregulation of ‘damaged DNA binding’ and ‘DNA repair’, *spt16*, *foxm1*, *bptf*, and *arpc5* were positively correlated with CO₂ treatment and activity traits, and *nit1*, whose loss of expression promotes resistance to DNA damage stress, was negatively correlated with CO₂ treatment and activity traits. Genes involved in protein

Table 6 Results across all three analysis methods in the CNS and eyes related to cellular stress

	DE		GSEA				WGCNA				
	Gene	CNS	Eyes	GO Term / Functional Category	CNS	Eyes	Gene	CNS		Eyes	
								CO ₂	Behaviour	CO ₂	Behaviour
Oxidative Stress											
Antioxidant and ROS production	<i>tf</i>	↑					<i>tf, scl4a11</i>	↑	↑		
	<i>cyb561d2</i>	↓		‘glutathione metabolic process’	↓						
	<i>cbs</i>		↑								
DNA damage and repair	<i>chrac1</i>	↑		‘damaged DNA binding’, ‘DNA repair’	↑		<i>spt16, foxm1, bptf, arpc5</i>	↑	↑		
							<i>nit1</i>	↓	↓		
Protein damage and ER stress	<i>ykt6</i>	↑	↑	‘endoplasmic reticulum’, ‘endoplasmic reticulum membrane’, ‘protein ubiquitination’, ‘protein deubiquitination’, ‘ubiquitin binding’, ‘ubiquitin-dependent protein catabolic process’, ‘thiol-dependent ubiquitin-specific protease activity’	↑	↑	<i>hspa5</i>	↑	↑		
				‘proteasome complex’	↑	↑					
				‘peptide metabolic process’		↑					
Cellular stress-induced apoptosis	<i>syvn1-b</i>	↑		‘regulation of apoptotic process’	↑		<i>apbb5, tmem214-b</i>	↑	↑		

Genes identified as significantly differentially expressed (DE) between current-day and elevated CO₂ conditions, GO Terms/functional categories significantly affected by elevated CO₂ treatment as identified by gene set enrichment analysis (GSEA), and genes identified as correlated with both CO₂ treatment and one or more OA-affected behaviours by weighted gene co-expression network analysis (WGCNA). See Table 2 for a description of the symbols

damage control and endoplasmic reticulum stress were also affected by CO₂ treatment; *ykt6*, which is essential for autophagy was upregulated in the CNS and eyes, and the heat shock protein *hspa5*, which is a key repressor of the unfolded protein response was positively correlated with CO₂ treatment and activity traits. Furthermore, genes that induce apoptosis in response to DNA damage (*apbb5*) and ER stress (*tmem214-b*), were positively correlated with CO₂ treatment and activity traits. There was also small, coordinated upregulation in the CNS of genes involved in the 'regulation of apoptotic process'.

Discussion

As the nervous system forms the fundamental link between animals and the environments they inhabit [3, 4], understanding the neurobiological impacts of environmental change is key to predicting how and why animals will respond to anthropogenic climate change. In this study, we sought to understand how projected end-of-century CO₂ levels alter the nervous system at a molecular level, and how such changes may affect behaviour of the whole animal. To do this, we investigated the transcriptomic response to ocean acidification (OA) of the central and peripheral nervous system of a marine invertebrate with a complex nervous system, the two-toned pygmy squid *Idiosepius pygmaeus*. We then correlated patterns of gene expression with CO₂ treatment levels and OA-affected behaviours in the same individuals. The central nervous system (CNS) and eyes of *I. pygmaeus* responded to elevated CO₂ with significant differential expression (DE) of a small number of genes, and widespread small but coordinated changes of genes belonging to important functional categories between CO₂ conditions. Furthermore, we identified 169 genes in the CNS, six genes in the eyes and ten genes in both tissues that were correlated with CO₂ treatment and one or more behaviours affected by OA, indicating these genes potentially contribute to OA-induced behavioural changes.

The GABA hypothesis is the predominant mechanistic explanation for OA-induced behavioural changes in fish [15, 77] and may also apply to marine invertebrates [10]. Pharmacological work has supported the GABA hypothesis in marine molluscs [17, 19], including in *I. pygmaeus* [18]. In the whole-body of a pteropod mollusc, a GABA_A receptor transcript was upregulated after OA exposure [32]. In fish nervous tissue, OA exposure has variable effects on GABA_A R subunit transcript expression, causing upregulation in some species [26, 30] but not another [31]. Furthermore, differences in OA exposure duration [25, 26, 28] and magnitude [29] are associated with variable effects on the expression of genes coding for GABA_A R subunits within species. In *I. pygmaeus*, we found small, coordinated downregulation in the CNS

and upregulation in the eyes of genes for ion-channel receptors, which included GABA_A receptor subunit transcripts. In the CNS, there was also upregulation of *syvn1-b* (implicated in GABA_Aα1 receptor subunit degradation [78, 79]), regulators of GABAergic neurotransmission were positively correlated with CO₂ treatment and behaviours (*phf24*, *rac1*), and *aldh5a1* (involved in the final degradation step of GABA [64]) was negatively correlated with CO₂ treatment and behaviours. Together, this data suggests an effect of OA on GABAergic signalling may be widespread, occurring not only in fish but also marine molluscs, however, effects may be species and tissue-specific.

Recent research suggests that various other types of neurotransmission may also be affected by OA and potentially contribute to consequent behavioural responses. Pharmacological research has identified altered function of a range of different types of ligand-gated Cl⁻ channels in *I. pygmaeus* [18] and the dopamine D1 receptor in a damselfish [80] contributing to OA-induced behavioural changes. Elevated CO₂ upregulated glycinergic, cholinergic and glutamatergic transcripts in the whole body of a pteropod mollusc [32], upregulated glutamatergic transcripts in the non-nervous tissue of oysters [81, 82], and altered acetylcholine receptor transcript expression in the whole body of another pteropod mollusc [33]. In fish nervous tissue, exposure to OA conditions caused upregulation of genes coding for glutamatergic and cholinergic neurotransmission of some species [26, 30, 31], but downregulation in others [21, 28]. In *I. pygmaeus*, we identified small, coordinated downregulation in the CNS and upregulation in the eyes of genes involved in neurotransmission mediated by ligand-gated ion channels, including transcripts for subunits of ionotropic glutamate, glycine and acetylcholine receptors. There was also small, coordinated downregulation in the CNS of G protein-coupled receptor (GPCR)-mediated neurotransmission, including genes for subunits of metabotropic glutamate, serotonin, dopamine and GABA (GABA_B) receptors. Key genes for glutamatergic and monoaminergic signalling were DE, and a subunit of nicotinic acetylcholine receptors (*chrna10*) was correlated with CO₂ treatment and behaviours in both tissues. Overall, this suggests that OA not only impacts GABA_A R function, but various different types of neurotransmission mediated by ligand-gated ion channels and GPCRs. However, as with GABAergic signalling, OA effects on other types of neurotransmission may vary by species and tissue type, and possibly other factors such as the magnitude and duration of OA exposure. Further experimentation is needed to understand how OA-induced transcriptomic responses translate to neurotransmission function and behaviour.

Genes involved in the general processes required for synaptic neurotransmission were attenuated in the CNS of *I. pygmaeus* after OA exposure, including Ca^{2+} , K^{+} and Na^{+} ion channels required for maintenance of membrane potential, action potential generation and neurotransmitter release. There was also a negative correlation between the expression of genes regulating synaptic neurotransmission with CO_2 treatment and activity traits. Genes for Ca^{2+} and K^{+} transporters and the regulation of neurotransmitter release were also downregulated in the brain of spiny damselfish collected from CO_2 seeps [28], but upregulated after acute and developmental OA exposure [26], and in fish olfactory tissue after short-term [31] and transgenerational OA exposure [30]. These transcriptomic signatures suggest an even more widespread effect of OA on neurotransmission, potentially altering the general processes required for synaptic neurotransmission to occur. However, experimentation is required to determine functional effects.

Neuroplasticity is the ability of the nervous system to change. Both neurogenesis (the process by which new neurons are generated and integrated into existing neural circuits) and synaptic plasticity (changing of synaptic strength over time) contribute to neuroplasticity [83]. In the CNS of *I. pygmaeus* we found small, coordinated upregulation and positive correlation with CO_2 treatment and activity traits of genes involved in all the stages required for neurogenesis (re-entering and exiting the cell cycle, cell proliferation and differentiation to form new neurons, and neural wiring involving cell migration and adhesion for new neurons to be incorporated into existing circuits). Widespread upregulation and positive correlations with CO_2 treatment and behaviours of genes in the CNS of *I. pygmaeus* involved in transcription, RNA processing, and protein processing could potentially be a response to deal with the changed protein demand required due to increased neuroplasticity. Notably, *cdk10*, which plays an important role in neurogenesis [84] was identified as correlated with the OA-induced increase in exploratory interactions in both the CNS and eyes. Genes involved in synaptogenesis (the formation of new synapses) and synaptic plasticity were also positively correlated with CO_2 treatment and OA-affected behaviours in the CNS of *I. pygmaeus*.

Despite not assessing the nervous tissue specifically, transcripts involved in neuronal cell adhesion, neuronal differentiation and survival and synaptic plasticity were also upregulated in the whole body of a pteropod mollusc after OA exposure [32]. In fish nervous tissue, genes involved in neurogenesis were upregulated in some species but not others [22], and genes involved in synaptic plasticity were upregulated in some species [26, 30], but downregulated in another species [21]. Thus, OA-induced transcriptomic responses related to

neuroplasticity may be widespread, occurring in fish and marine molluscs. However, this response may be tax-specific and/or could be affected by differences in CO_2 exposure duration and magnitude that have differed between studies.

Elevated CO_2 alters the molluscan immune response, with most research focusing on bivalves [85–89]), though the immune response of an octopus was also affected by elevated CO_2 [90]. Here, we found DE of genes that regulate immune signal transduction pathways and which are also implicated in the molluscan immune response (*map4k5/3*, *syvn1-b*, *psenen*, *cbs*) [73, 91–93]. There were also changes in expression of a range of genes that code for immune effectors, including iron sequestration (*tf* and *cbs*), autophagy (*map1l3ca/b*), controlling the pool of available nucleoside triphosphates (*nme6*), and phagocytosis ('cell adhesion' and multiple cytoskeleton functional categories). Previous research has also indicated altered phagocytosis in molluscs at elevated CO_2 ; adhesion capacity of haemocytes was decreased in a clam and expression of integrin (involved in cell adhesion for phagocytosis) was decreased in an oyster species [94] and increased in another oyster [81]. Furthermore, the phagocytic rate and cytoskeleton component abundance was decreased, and the expression of cytoskeleton genes was upregulated, in a clam at elevated CO_2 [87]. Our results show an effect of OA on the transcriptional profile of genes implicated in the immune response suggesting OA-induced alterations in immune function may also occur in molluscan nervous tissue, though further research directly measuring immune function within the nervous system is required.

Cross-talk between the neuroendocrine and immune systems coordinates appropriate physiological and behavioural responses to environmental change [95]. In molluscs, neuronal release of norepinephrine regulates immune responses through a neuroendocrine-immune axis-like pathway [96]. Specifically, changes in the expression and activity of *maoa* (upregulated in *I. pygmaeus* eyes here) plays a key role in immune functioning via norepinephrine in molluscs [66–68]. Immune-derived factors can also feedback to alter the nervous system and behaviour [97, 98]. Indeed, *tf*, which is a key component of the molluscan innate immune response (Lambert et al., 2005; Ong et al., 2006; Herath et al., 2015; Salazar et al., 2015; Li et al., 2019) was upregulated and positively correlated with CO_2 treatment and activity traits in the CNS of *I. pygmaeus*. We also found the expression of genes coding for integrins *itga4* and *itga9*, cell adhesion molecules playing a key role in invertebrate immune responses (Johansson, 1999; Terahara et al., 2006), were positively correlated in the CNS with CO_2 treatment and activity traits. Therefore, it is possible that OA-induced changes in neurotransmission could have consequences

on immune function, and changes in immune function could also feedback on the nervous system to alter behaviours at elevated CO₂. However, the potential links between OA, neurotransmission, immune function and behaviour remain to be experimentally tested.

Oxidative stress occurs when there is an imbalance between the production of reactive oxygen species (ROS) and protection by antioxidant mechanisms [99]. Elevated CO₂ induces oxidative stress in molluscs, increasing ROS and altering antioxidant defences inducing DNA damage, lipid peroxidation and apoptosis [100–105]. In *I. pygmaeus*, we found DE of genes implicated in the production of antioxidants, including ascorbate and glutathione. We also identified upregulation in the CNS of genes involved in DNA damage and repair, protein damage and endoplasmic reticulum stress, and cellular stress-induced apoptosis. In molluscs, OA exposure has previously been shown to result in DNA damage [100, 106] and increased apoptosis [100, 104].

The nervous system is particularly vulnerable to oxidative stress [107, 108] and oxidative stress-induced damage within the nervous system can disrupt neurotransmission and neuronal function [99, 108–110]. In mammals, a link between oxidative stress in the nervous system and changes in behaviour has been demonstrated [111–113]. In the CNS of *I. pygmaeus*, we identified a positive correlation between the expression of genes implicated in oxidative stress and CO₂ treatment and OA-affected behaviours. In the eyes, two genes (*crb* and *zranb1*) potentially correlated with OA-induced behavioural alterations of *I. pygmaeus* are implicated in oxidative-stress induced retinal degeneration [114, 115]. In particular, *crb* prevents photoreceptor degeneration by limiting the production of ROS and the resultant oxidative damage [114]. A recent study in a cuttlefish found the behavioural effects of OA were associated with an altered retinal structure and an increase in apoptotic cells within the eyes [116]. Thus, it's possible that OA-induced oxidative stress could contribute to behavioural alterations at elevated CO₂, potentially through central and peripheral mechanisms, but further electrophysiological and whole-animal behavioural experimentation is required.

When interpreting our results, there are a few important things to consider. Firstly, despite the reasonable assumption that changes in gene expression driving behavioural responses occur prior to behavioural production [117], we measured gene expression immediately after the OA-induced behavioural responses in *I. pygmaeus* due to the necessity of terminal sampling to obtain nervous tissue. Furthermore, the process of transcribing genes is far too slow to mediate rapid behavioural responses, which are instead mediated by fast electrical signals passed along and between neurons [117]. Thus, our transcriptomic results do not describe

the neuronal mechanisms driving the immediate behavioural responses to a stimulus, but rather those that likely contribute to longer-term changes in behaviour [117, 118] in OA conditions. Secondly, organism responses to OA can be sex-specific [119], including marine invertebrate behavioural responses [120, 121]. We used males only in this study. Future research could consider using both sexes to determine whether behavioural responses to OA are sex-specific, and if so whether differing transcriptional profiles underly these sex-specific responses.

Conclusion

Here, we demonstrate differential expression of specific genes and widespread small but coordinated changes in expression of genes belonging to relevant functional categories in the CNS and eyes following short-term exposure of male *I. pygmaeus* to OA. We also report genes correlated with both CO₂ treatment and OA-affected behaviours, indicating these genes as potentially correlated with CO₂-induced behavioural change in *I. pygmaeus*. The results identify alterations in the transcriptional profile of genes implicated in neurotransmission, neuroplasticity, immune function and oxidative stress. These molecular changes may contribute to OA-induced behavioural change, as suggested by correlations between gene expression profiles, CO₂ treatment and OA-affected behaviours. Our results build on existing knowledge and provide novel hypotheses for future experiments, including electrophysiological and behavioural tests, to determine the range of processes responsible for behavioural changes in marine animals exposed to projected future OA conditions.

Supplementary Information

The online version contains supplementary material available at <https://doi.org/10.1186/s12864-024-10542-5>.

Supplementary Material 1

Supplementary Material 2

Supplementary Material 3

Supplementary Material 4

Acknowledgements

We thank the technical staff at James Cook University Marine and Aquaculture Facilities Unit (Ben Lawes, Simon Wever and Andrew Thompson), and Annam Raza, Natalie Swinhoe and Michael Jarrold for assistance with the live animal work. We also thank the Breakwater Marina, Townsville for permission to collect animals within their premises. Thank you to Carolyn Smith-Keune and Paul O'Brien for molecular laboratory support and Taewoo Ryu for advice on the computational analysis. We are grateful for the support provided by the Scientific Computing and Data Analysis section of Research Support Division at Okinawa Institute of Science and Technology Graduate University.

Author contributions

JT: Conceptualisation, Methodology, Software, Formal analysis, Investigation, Resources, Data curation, Writing - original draft, Writing - review and editing, Visualisation. RH: Methodology, Software, Writing - review and editing. CS:

Conceptualisation, Methodology, Resources, Writing - review and editing. S-AW: Conceptualisation, Resources, Writing - review and editing, Supervision. PM: Conceptualisation, Resources, Writing - review and editing, Supervision. TR: Conceptualisation, Methodology, Resources, Writing - review and editing, Supervision.

Funding

This work was supported by the Australian Research Council Centre of Excellence for Coral Reef Studies (PLM, S-AW), an Australian Government Research Training Program Scholarship (JTT) and the Okinawa Institute of Science and Technology Graduate University (TR, RH, JTT).

Data availability

The datasets supporting the conclusions of this article are available in the National Centre for Biotechnology Information (NCBI) and Research Data JCU repositories. Raw RNA-sequencing and ISO-sequencing data, and the transcriptome assembly (fasta file) can be found at NCBI BioProject PRJNA798187. Raw gene count data, raw water sampling data, all scripts used for bioinformatic analyses, the annotated transcriptome assembly (OmicsBox and csv files), R code used for the statistical analyses (differential expression and gene set analyses), and data files to accompany the statistical analyses are available from the Research Data JCU repository at DOI 10.25903/ha66-mm11. All R code for the statistical analyses (correlating gene expression profiles with CO₂ treatment and OA-affected behaviours), as well as accompanying data files for the statistical analyses, can be found at the Research Data JCU repository at DOI 10.25903/7dcz-th66.

Declarations

Ethical approval

This study was approved by and followed the animal ethics guidelines at James Cook University (JCU animal ethics number A2644).

Consent for publication

Not applicable.

Competing interests

The authors declare no competing interests.

Received: 1 April 2024 / Accepted: 20 June 2024

Published online: 25 June 2024

References

- Fuller A, Dawson T, Helmuth B, Hetem Robyn S, Mitchell D, Maloney Shane K. Physiological mechanisms in coping with climate change. *Physiol Biochem Zool.* 2010;83(5):713–20.
- Cooke SJ, Sack L, Franklin CE, Farrell AP, Beardall J, Wikelski M, et al. What is conservation physiology? Perspectives on an increasingly integrated and essential science. *Conserv Physiol.* 2013;1(1):cot001.
- Kelley J, Chapuis L, Davies WIL, Collin S. Sensory system responses to human-induced environmental change. *Front Ecol Evol.* 2018;6:95.
- O'Donnell S. The neurobiology of climate change. *Sci Nat.* 2018;105(1):1–7.
- Bindoff NL, Cheung WW, Kairo JG, Arístegui J, Guinder VA, Hallberg R, et al. Changing ocean, marine ecosystems, and dependent communities. In: Pörtner H-O, Roberts D, Masson-Delmotte V, Zhai P, Tignor M, Poloczanska E, et al. editors. IPCC Special Report on the Ocean and Cryosphere in a changing climate. Cambridge, UK and New York, NY, USA: Cambridge University Press; 2019. pp. 447–587.
- Doney SC, Fabry VJ, Feely RA, Kleypas JA. Ocean acidification: the other CO₂ problem. *Annual Rev Mar Sci.* 2009;1(1):169–92.
- Pörtner H-O, Langenbuch M, Reipschläger A. Biological impact of elevated ocean CO₂ concentrations: lessons from animal physiology and earth history. *J Oceanogr.* 2004;60(4):705–18.
- Kroeker KJ, Kordas RL, Crim RN, Singh GG. Meta-analysis reveals negative yet variable effects of ocean acidification on marine organisms. *Ecol Lett.* 2010;13(11):1419–34.
- Nagelkerken I, Connell SD. Global alteration of ocean ecosystem functioning due to increasing human CO₂ emissions. *Proceedings of the National Academy of Sciences.* 2015;112(43):13272–7.
- Thomas J, Munday P, Watson S-A. Toward a mechanistic understanding of marine invertebrate behaviour at elevated CO₂. *Front Mar Sci.* 2020;7:345.
- Durant A, Khodikian E, Porteus CS. Ocean acidification alters foraging behaviour in Dungeness crab through impairment of the olfactory pathway. *Global Change Biol.* 2023;n/a(n/a).
- Chen EY-S. Often overlooked: understanding and meeting the current challenges of marine invertebrate conservation. *Front Mar Sci.* 2021;8(1161):690704.
- Bertness MD, Gaines SD, Hay ME. *Marine Community Ecology.* Sunderland, Massachusetts: Sinauer Associates; 2001.
- Nagelkerken I, Munday PL. Animal behaviour shapes the ecological effects of ocean acidification and warming: moving from individual to community-level responses. *Global Change Biol.* 2015;22(3):974–89.
- Nilsson GE, Dixon DL, Domenici P, McCormick MI, Sørensen C, Watson S-A, et al. Near-future carbon dioxide levels alter fish behaviour by interfering with neurotransmitter function. *Nat Clim Change.* 2012;2(3):201–4.
- Heuer RM, Hamilton TJ, Nilsson GE. The physiology of behavioural impacts of high CO₂. In: Grosell M, Munday PL, Farrell AP, Brauner CJ, editors. *Carbon Dioxide. Fish Physiology.* 37. Cambridge. San Diego, Oxford, London: Academic; 2019. pp. 161–94.
- Watson S-A, Lefevre S, McCormick MI, Domenici P, Nilsson GE, Munday PL. Marine mollusc predator-escape behaviour altered by near-future carbon dioxide levels. *Proc Royal Soc Lond B: Biol Sci.* 2014;281(1774):20132377.
- Thomas JT, Spady BL, Munday PL, Watson S-A. The role of ligand-gated chloride channels in behavioural alterations at elevated CO₂ in a cephalopod. *J Exp Biol.* 2021;224(13):jeb242335.
- Clements JC, Bishop MM, Hunt HL. Elevated temperature has adverse effects on GABA-mediated avoidance behaviour to sediment acidification in a wide-ranging marine bivalve. *Mar Biol.* 2017;164(3):56.
- Charpentier CL, Cohen JH. Acidification and γ -aminobutyric acid independently alter kairomone-induced behaviour. *Open Sci.* 2016;3(9):160311.
- Porteus CS, Hubbard PC, Webster TMU, van Aerle R, Canário AV, Santos EM, et al. Near-future CO₂ levels impair the olfactory system of a marine fish. *Nat Clim Change.* 2018;8(8):737–46.
- Lai F, Fagernes CE, Bernier NJ, Miller GM, Munday PL, Jutfelt F, et al. Responses of neurogenesis and neuroplasticity related genes to elevated CO₂ levels in the brain of three teleost species. *Biol Lett.* 2017;13(8):20170240.
- Strader ME, Wong JM, Hofmann GE. Ocean acidification promotes broad transcriptomic responses in marine metazoans: a literature survey. *Front Zool.* 2020;17(1):7.
- Schunter C, Ravasi T, Munday PL, Nilsson GE. Neural effects of elevated CO₂ in fish may be amplified by a vicious cycle. *Conserv Physiol.* 2019;7(1):coz100.
- Schunter C, Welch MJ, Ryu T, Zhang H, Berumen ML, Nilsson GE, et al. Molecular signatures of transgenerational response to ocean acidification in a species of reef fish. *Nat Clim Change.* 2016;6:1014–8.
- Schunter C, Welch MJ, Nilsson GE, Rummer JL, Munday PL, Ravasi T. An interplay between plasticity and parental phenotype determines impacts of ocean acidification on a reef fish. *Nat Ecol Evol.* 2018;2(2):334.
- Schunter C, Jarrold MD, Munday PL, Ravasi T. Diel pCO₂ fluctuations alter the molecular response of coral reef fishes to ocean acidification conditions. *Mol Ecol.* 2021;30:5105–18.
- Kang J, Nagelkerken I, Rummer JL, Rodolfo-Metalpa R, Munday PL, Ravasi T, et al. Rapid evolution fuels transcriptional plasticity to ocean acidification. *Global Change Biol.* 2022;00:1–16.
- Toy JA, Kroeker KJ, Logan CA, Takeshita Y, Longo GC, Bernardi G. Upwelling-level acidification and pH/pCO₂ variability moderate effects of ocean acidification on brain gene expression in the temperate surfperch, *Embiotoca jacksoni*. *Mol Ecol.* 2022;31(18):4707–25.
- Cohen-Rengifo M, Danion M, Gonzalez A-A, Bégout M-L, Cormier A, Noël C, et al. The extensive transgenerational transcriptomic effects of ocean acidification on the olfactory epithelium of a marine fish are associated with a better viral resistance. *BMC Genomics.* 2022;23(1):448.
- Williams CR, Dittman AH, McElhany P, Busch DS, Maher MT, Bammler TK, et al. Elevated CO₂ impairs olfactory-mediated neural and behavioral responses and gene expression in ocean-phase coho salmon (*Oncorhynchus kisutch*). *Global Change Biol.* 2019;25:963–77.
- Moya A, Howes EL, Lacoue-Labarthe T, Forêt S, Hanna B, Medina M, et al. Near-future pH conditions severely impact calcification, metabolism and the nervous system in the pteropod *Heliconoides Inflatus*. *Global Change Biol.* 2016;22(12):3888–900.

33. Johnson KM, Hofmann GE. Transcriptomic response of the Antarctic pteropod *Limacina helicina Antarctica* to ocean acidification. *BMC Genomics*. 2017;18(1):812.
34. Steenstrup J. Sepiadiarium Og Idiosepius to Nye Slaegter Af Sepiernes Familie. Med Bemaerkninger Om De to beslaegtede former Sepiolidea D'Orb. Og Spirula Lmk. Danske Videnskabernes Selskabs Skrifter 6 Raekke Naturvidenskabelig Og Mathematisk. 1881;1(3):211–42.
35. Hanlon RT, Messenger JB. *Cephalopod Behaviour*. Second ed. Cambridge: Cambridge University Press; 2018.
36. Reid A. Family Idiosepiidae. In: Jereb P, Roper CFE, editors. *Cephalopods of the World: An Annotated and Illustrated Catalogue of Cephalopod species known to date volume 1 Chambered nautilus and sepioids (Nautilidae, Sepiidae, Sepiolidae, Sepiariidae, Idiosepiidae and Spirulidae)*. FAO species catalogue for fishery purposes. Volume 1. Rome: FAO; 2005. pp. 208–10.
37. Moynihan M. Notes on the behavior of *Idiosepius pygmaeus* (Cephalopoda; Idiosepiidae). *Behaviour*. 1983;85(1):42–57.
38. Jackson GD. The use of statolith microstructures to analyze life history events in the small tropical cephalopod *Idiosepius pygmaeus*. *Fish Bull*. 1988;87:265–72.
39. Spady BL, Watson S-A, Chase TJ, Munday PL. Projected near-future CO₂ levels increase activity and alter defensive behaviours in the tropical squid *Idiosepius pygmaeus*. *Biol Open*. 2014;3(11):1063–70.
40. Spady BL, Munday PL, Watson S-A. Predatory strategies and behaviours in cephalopods are altered by elevated CO₂. *Global Change Biol*. 2018;24:2585–96.
41. Mather JA. Behaviour development: a cephalopod perspective. *Int J Comp Psychol*. 2006;19(1):98–115.
42. Muntz WRA. Visual systems, behaviour, and environment in cephalopods. In: Archer SN, Djamgoz MBA, Loew ER, Partridge JC, Vallergera S, editors. *Adaptive mechanisms in the Ecology of Vision*. Dordrecht: Springer Netherlands; 1999. pp. 467–83.
43. Chung W-S, Kurniawan ND, Marshall NJ. Comparative brain structure and visual processing in octopus from different habitats. *Curr Biol*. 2022;32(1):97–e1104.
44. Hannan KD, Miller GM, Watson S-A, Rummer JL, Fabricius K, Munday PL. Diel pCO₂ variation among coral reefs and microhabitats at Lizard Island, Great Barrier Reef. *Coral Reefs*. 2020;39(5):1391–406.
45. Andrews S. FastQC: A quality control tool for high throughput sequence data. <https://www.bioinformatics.babraham.ac.uk/projects/fastqc/2010>.
46. Ewels P, Magnusson M, Lundin S, Källner M, MultiQC. Summarize analysis results for multiple tools and samples in a single report. *Bioinformatics*. 2016;32(19):3047–8.
47. Chen S, Zhou Y, Chen Y, Gu J. Fastp: an ultra-fast all-in-one FASTQ preprocessor. *Bioinformatics*. 2018;34(17):i884–90.
48. Wood DE, Lu J, Langmead B. Improved metagenomic analysis with Kraken 2. *Genome Biol*. 2019;20(1):257.
49. Thomas JT, Huerlimann R, Schunter C, Watson S-A, Munday PL, Ravasi T. Two-toned pygmy squid (*Idiosepius pygmaeus*) transcriptome assembly, and transcriptomic response of the nervous system to elevated CO₂. National Centre for Biotechnology Information. BioProject: PRJNA798187. 2022.
50. Thomas JT, Huerlimann R, Schunter C, Watson S-A, Munday PL, Ravasi T. Two-toned pygmy squid (*Idiosepius pygmaeus*) transcriptome assembly, and transcriptomic response of the nervous system to elevated CO₂. James Cook University. <https://doi.org/10.25903/ha66-mm11>. 2024.
51. Patro R, Duggal G, Love MI, Irizarry RA, Kingsford C. Salmon provides fast and bias-aware quantification of transcript expression. *Nat Methods*. 2017;14(4):417–9.
52. Davidson NM, Oshlack A, Corset. Enabling differential gene expression analysis for *de novo* assembled transcriptomes. *Genome Biol*. 2014;15(7):1–14.
53. R Core Team. R: A language and environment for statistical computing. Vienna, Austria: R Foundation for Statistical Computing. 2021.
54. RStudio Team. RStudio: Integrated development environment for R. Boston, MA: RStudio; PBC. 2021.
55. Love MI, Huber W, Anders S. Moderated estimation of Fold change and dispersion for RNA-seq data with DESeq2. *Genome Biol*. 2014;15(12):550.
56. Stephens M. False discovery rates: a new deal. *Biostatistics*. 2016;18(2):275–94.
57. Yu G, Wang L-G, Han Y, He Q-Y, clusterProfiler. An R package for comparing biological themes among gene clusters. *OMICS*. 2012;16(5):284–7.
58. Shannon P, Markiel A, Ozier O, Baliga NS, Wang JT, Ramage D, et al. Cytoscape: A software environment for integrated models of biomolecular interaction networks. *Genome Res*. 2003;13(11):2498–504.
59. Merico D, Isserlin R, Stueker O, Emili A, Bader GD. Enrichment map: a network-based method for gene-set enrichment visualization and interpretation. *PLoS ONE*. 2010;5(11):e13984.
60. Langfelder P, Horvath S. WGCNA: an R package for weighted correlation network analysis. *BMC Bioinformatics*. 2008;9(1):1–13.
61. González I, Déjean S, Martin P, Baccini A. CCA: an R package to extend canonical correlation analysis. *J Stat Softw*. 2008;23(12):1–14.
62. Fuller TF, Ghazalpour A, Aten JE, Drake TA, Lusis AJ, Horvath S. Weighted gene coexpression network analysis strategies applied to mouse weight. *Mamm Genome*. 2007;18(6):463–72.
63. Horvath S, Dong J. Geometric interpretation of gene coexpression network analysis. *PLoS Comput Biol*. 2008;4(8):e1000117–e.
64. Kim Y-G, Lee S, Kwon O-S, Park S-Y, Lee S-J, Park B-J, et al. Redox-switch modulation of human SSADH by dynamic catalytic loop. *EMBO J*. 2009;28(7):959–68.
65. Guen VJ, Gamble C, Lees JA, Colas P. The awakening of the CDK10/Cyclin M protein kinase. *Oncotarget*. 2017;8(30):50174–86.
66. Zhou Z, Wang L, Gao Y, Wang M, Zhang H, Wang L, et al. A monoamine oxidase from scallop *Chlamys farreri* serving as an immunomodulator in response against bacterial challenge. *Dev Comp Immunol*. 2011;35(7):799–807.
67. Sun Q, Zheng Y, Chen X, Kong N, Wang Y, Zhang Y et al. A diet rich in diatom improves the antibacterial capacity of Pacific oyster *Crassostrea gigas* by enhancing norepinephrine-regulated immunomodulation. *Invertebrate Survival J*. 2021:56–65.
68. Liu Z, Wang L, Lv Z, Zhou Z, Wang W, Li M, et al. The cholinergic and adrenergic autocrine signaling pathway mediates immunomodulation in oyster *Crassostrea gigas*. *Front Immunol*. 2018;9(284):284.
69. Lambert LA, Perri H, Halbrooks PJ, Mason AB. Evolution of the transferrin family: conservation of residues associated with iron and anion binding. *Comp Biochem Physiol B: Biochem Mol Biol*. 2005;142(2):129–41.
70. Ong ST, Shan Ho JZ, Ho B, Ding JL. Iron-withholding strategy in innate immunity. *Immunobiology*. 2006;211(4):295–314.
71. Herath HMLPB, Elvitigala DAS, Godahewa GI, Whang I, Lee J. Molecular insights into a molluscan transferrin homolog identified from disk abalone (*Haliotis discus discus*) evidencing its detectable role in host antibacterial defense. *Dev Comp Immunol*. 2015;53(1):222–33.
72. Li H-W, Chen C, Kuo W-L, Lin C-J, Chang C-F, Wu G-C. The characteristics and expression profile of transferrin in the accessory nidamental gland of the bigfin reef squid during bacteria transmission. *Sci Rep*. 2019;9(1):20163.
73. Salazar KA, Joffe NR, Dinguirard N, Houde P, Castillo MG. Transcriptome analysis of the white body of the squid *Euprymna tasmanica* with emphasis on immune and hematopoietic gene discovery. *PLoS ONE*. 2015;10(3):e0119949.
74. Han Z, Wang W, Lv X, Zong Y, Liu S, Liu Z, et al. ATG10 (autophagy-related 10) regulates the formation of autophagosome in the anti-virus immune response of pacific oyster (*Crassostrea gigas*). *Fish Shellfish Immunol*. 2019;91:325–32.
75. Moreau P, Moreau K, Segarra A, Tourbiez D, Travers M-A, Rubinsztein DC, et al. Autophagy plays an important role in protecting Pacific oysters from OsHV-1 and *Vibrio aestuarianus* infections. *Autophagy*. 2015;11(3):516–26.
76. Picot S, Morga B, Faury N, Chollet B, Dégremont L, Travers M-A, et al. A study of autophagy in hemocytes of the Pacific oyster, *Crassostrea gigas*. *Autophagy*. 2019;15(10):1801–9.
77. Tresguerres M, Hamilton TJ. Acid-base physiology, neurobiology and behaviour in relation to CO₂-induced ocean acidification. *J Exp Biol*. 2017;220(12):2136–48.
78. Crider A, Pandya CD, Peter D, Ahmed AO, Pillai A. Ubiquitin-proteasome dependent degradation of GABA_Aα1 in autism spectrum disorder. *Mol Autism*. 2014;5(1):45.
79. Jiao D, Chen Y, Liu Y, Ju Y, Long J, Du J et al. SYVN1, an ERAD E3 ubiquitin ligase, is involved in GABA_Aα1 degradation associated with methamphetamine-induced conditioned place preference. *Front Mol Neurosci*. 2017;10(313).
80. Hamilton TJ, Tresguerres M, Kwan GT, Szaskiewicz J, Franczak B, Cyrokkak T et al. Effects of ocean acidification on dopamine-mediated behavioral responses of a coral reef damselfish. *Sci Total Environ*. 2023:162860.
81. Ertl NG, O'Connor WA, Wiegand AN, Elizur A. Molecular analysis of the Sydney rock oyster (*Saccostrea Glomerata*) CO₂ stress response. *Clim Change Responses*. 2016;3(1):6.
82. Wang X, Wang M, Wang W, Liu Z, Xu J, Jia Z, et al. Transcriptional changes of Pacific oyster *Crassostrea gigas* reveal essential role of calcium signal pathway in response to CO₂-driven acidification. *Sci Total Environ*. 2020;741:140177.

83. Costandi M, Neuroplasticity. Cambridge, Massachusetts: The MIT Press; 2016.
84. Yeh C-W, Kao S-H, Cheng Y-C, Hsu L-S. Knockdown of cyclin-dependent kinase 10 (*cdk10*) gene impairs neural progenitor survival via modulation of *raf1a* gene expression. *J Biol Chem*. 2013;288(39):27927–39.
85. Liu S, Shi W, Guo C, Zhao X, Han Y, Peng C, et al. Ocean acidification weakens the immune response of blood clam through hampering the NF-kappa β and toll-like receptor pathways. *Fish Shellfish Immunol*. 2016;54:322–7.
86. Li S, Liu Y, Liu C, Huang J, Zheng G, Xie L, et al. Morphology and classification of hemocytes in *Pinctada fucata* and their responses to ocean acidification and warming. *Fish Shellfish Immunol*. 2015;45(1):194–202.
87. Su W, Rong J, Zha S, Yan M, Fang J, Liu G. Ocean acidification affects the cytoskeleton, lysozymes, and nitric oxide of hemocytes: a possible explanation for the hampered phagocytosis in blood clams, *Tegillarca Granosa*. *Front Physiol*. 2018;9(619).
88. Wu F, Lu W, Shang Y, Kong H, Li L, Sui Y, et al. Combined effects of seawater acidification and high temperature on hemocyte parameters in the thick shell mussel *Mytilus coruscus*. *Fish Shellfish Immunol*. 2016;56:554–62.
89. Bibby R, Widdicombe S, Parry H, Spicer J, Pipe R. Effects of ocean acidification on the immune response of the blue mussel *Mytilus edulis*. *Aquat Biology*. 2008;2(1):67–74.
90. Culler-Juarez ME, Onthank KL. Elevated immune response in *Octopus rubescens* under ocean acidification and warming conditions. *Mar Biol*. 2021;168(9):137.
91. Goodson MS, Kojadinovic M, Troll JV, Scheetz TE, Casavant TL, Soares MB, et al. Identifying components of the NF- κ B pathway in the beneficial *Euprymna scolopes-Vibrio fischeri* light organ symbiosis. *Appl Environ Microbiol*. 2005;71(11):6934–46.
92. Canesi L, Betti M, Ciacci C, Lorusso L, Pruzzo C, Gallo G. Cell signalling in the immune response of mussel hemocytes. *Invertebrate Survival J*. 2006;3(1):40–9.
93. De Zoysa M, Nikapitiya C, Oh C, Whang I, Lee J-S, Jung S-J, et al. Molecular evidence for the existence of lipopolysaccharide-induced TNF- α factor (LITAF) and Rel/NF- κ B pathways in disk abalone (*Haliotis discus discus*). *Fish Shellfish Immunol*. 2010;28(5):754–63.
94. Ivanina AV, Hawkins C, Sokolova IM. Immunomodulation by the interactive effects of cadmium and hypercapnia in marine bivalves *Crassostrea virginica* and *Mercenaria mercenaria*. *Fish Shellfish Immunol*. 2014;37(2):299–312.
95. Demas GE, Adamo SA, French SS. Neuroendocrine-immune crosstalk in vertebrates and invertebrates: implications for host defence. *Funct Ecol*. 2011;25(1):29–39.
96. Liu Z, Zhou Z, Jiang Q, Wang L, Yi Q, Qiu L, et al. The neuroendocrine immunomodulatory axis-like pathway mediated by circulating haemocytes in pacific oyster *Crassostrea gigas*. *Open Biology*. 2017;7(1):160289.
97. Dantzer R, Kelley KW. Twenty years of research on cytokine-induced sickness behavior. *Brain Behav Immun*. 2007;21(2):153–60.
98. Adamo SA. Comparative psychoneuroimmunology: evidence from the insects. *Behav Cogn Neurosci Rev*. 2006;5(3):128–40.
99. Halliwell B, Gutteridge J. Oxidative stress and redox regulation: adaptation, damage, repair, senescence, and death. In: Halliwell B, Gutteridge J, editors. *Free radicals in Biology and Medicine* Fifth Edition. Volume 3. Oxford University Press; 2015. pp. 199–283.
100. Cao R, Liu Y, Wang Q, Zhang Q, Yang D, Liu H et al. The impact of ocean acidification and cadmium on the immune responses of Pacific oyster, *Crassostrea gigas*. *Fish & Shellfish Immunology*. 2018;81:456–62.
101. Cao R, Wang Q, Yang D, Liu Y, Ran W, Qu Y, et al. CO₂-induced ocean acidification impairs the immune function of the Pacific oyster against *Vibrio splendidus* challenge: an integrated study from a cellular and proteomic perspective. *Sci Total Environ*. 2018;625:1574–83.
102. Tomanek L, Zuzow MJ, Ivanina AV, Beniash E, Sokolova IM. Proteomic response to elevated P_{CO2} level in eastern oysters, *Crassostrea virginica*. Evidence for oxidative stress. *J Exp Biol*. 2011;214(11):1836–44.
103. Wang Q, Cao R, Ning X, You L, Mu C, Wang C, et al. Effects of ocean acidification on immune responses of the Pacific oyster *Crassostrea gigas*. *Fish Shellfish Immunol*. 2016;49:24–33.
104. Zhang T, Qu Y, Zhang Q, Tang J, Cao R, Dong Z, et al. Risks to the stability of coral reefs in the South China Sea: an integrated biomarker approach to assess the physiological responses of *Trachus Niloticus* to ocean acidification and warming. *Sci Total Environ*. 2021;782:146876.
105. Kim MJ, Kim JA, Lee D-W, Park Y-S, Kim J-H, Choi CY. Oxidative stress and apoptosis in Disk Abalone (*Haliotis discus hannai*) caused by Water temperature and pH changes. *Antioxidants*. 2023;12(5):1003.
106. Nardi A, Benedetti M, d'Errico G, Fattorini D, Regoli F. Effects of ocean warming and acidification on accumulation and cellular responsiveness to cadmium in mussels *Mytilus galloprovincialis*: importance of the seasonal status. *Aquat Toxicol*. 2018;204:171–9.
107. Valko M, Leibfritz D, Moncol J, Cronin MT, Mazur M, Telser J. Free radicals and antioxidants in normal physiological functions and human disease. *Int J Biochem Cell Biol*. 2007;39(1):44–84.
108. Halliwell B. Oxidative stress and neurodegeneration: where are we now? *J Neurochem*. 2006;97(6):1634–58.
109. Bouayed J, Rammal H, Soulimani R. Oxidative stress and anxiety: relationship and cellular pathways. *Oxidative Med Cell Longev*. 2009;2:623654.
110. Lebel CP, Bondy SC. Oxygen radicals: common mediators of neurotoxicity. *Neurotoxicol Teratol*. 1991;13(3):341–6.
111. Rammal H, Bouayed J, Soulimani R. A direct relationship between aggressive behavior in the resident/intruder test and cell oxidative status in adult male mice. *Eur J Pharmacol*. 2010;627(1):173–6.
112. Bouayed J. Relationship between oxidative stress and anxiety: emerging role of antioxidants within therapeutic or preventive approaches. *Anxiety Disorders*. 2011:27–38.
113. Bhatt S, Nagappa AN, Patil CR. Role of oxidative stress in depression. *Drug Discovery Today*. 2020;25(7):1270–6.
114. Chartier FJ-M, Hardy É-L, Laprise P. Crumbs limits oxidase-dependent signaling to maintain epithelial integrity and prevent photoreceptor cell death. *J Cell Biol*. 2012;198(6):991–8.
115. Wang J-J, Shan K, Liu B-H, Liu C, Zhou R-M, Li X-M, et al. Targeting circular RNA-ZRANB1 for therapeutic intervention in retinal neurodegeneration. *Cell Death Dis*. 2018;9(5):540.
116. Xie J, Sun X, Li P, Zhou T, Jiang R, Wang X. The impact of ocean acidification on the eye, cuttlebone and behaviors of juvenile cuttlefish (*Sepiella inermis*). *Mar Pollut Bull*. 2023;190:114831.
117. Fischer EK, Hauber ME, Bell AM. Back to the basics? Transcriptomics offers integrative insights into the role of space, time and the environment for gene expression and behaviour. *Biol Lett*. 2021;17(9):20210293.
118. Clayton DF, Anreiter I, Aristizabal M, Frankland PW, Binder EB, Citri A. The role of the genome in experience-dependent plasticity: Extending the analogy of the genomic action potential. *Proceedings of the National Academy of Sciences*. 2020;117(38):23252–60.
119. Ellis RP, Davison W, Queirós AM, Kroeker KJ, Calosi P, Dupont S, et al. Does sex really matter? Explaining intraspecific variation in ocean acidification responses. *Biol Lett*. 2017;13(2):20160761.
120. Marčeta T, Matozzo V, Alban S, Badocco D, Pastore P, Marin MG. Do males and females respond differently to ocean acidification? An experimental study with the sea urchin *Paracentrotus lividus*. *Environ Sci Pollut Res*. 2020:1–15.
121. Richardson B, Martin H, Bartels-Hardege H, Fletcher N, Hardege JD. The role of changing pH on olfactory success of predator–prey interactions in green shore crabs, *Carcinus maenas*. *Aquat Ecol*. 2021.
122. Thomas JT, Huerlimann R, Schunter C, Watson S-A, Munday PL, Ravasi T. Correlating gene expression profiles with CO₂ treatment and OA-affected behaviours in the two-toned pygmy squid (*Idiosepius pygmaeus*). James Cook University. <https://doi.org/10.25903/7dzc-th66>. 2024.

Publisher's Note

Springer Nature remains neutral with regard to jurisdictional claims in published maps and institutional affiliations.